

UNANNOUNCED

AD-A956 154

DTIC
ELECTED
FEB 16 1993

DETERMINATION OF DISCHARGE
AND THRUST COEFFICIENTS OF A
CHOKED ASME NOZZLE FROM
EXIT FLOW SURVEYS
(ADDITIONAL TESTS)

by

James S. Holdhusen
Donald Perusse

Conducted for
General Electric Company
Cincinnati, Ohio

G. E. Purchase Order No. 200G230285
FluiDyne Project 0470

September 1965

Approved by:

James L. Grunnet
James L. Grunnet
Project Engineer

Nicholas C. Helm
Nicholas C. Helm
Program Planner

Owen P. Lamb
Owen P. Lamb
Program Manager

93-02792

DISTRIBUTION STATEMENT A	
Approved for public release Distribution Unlimited	

108

93

FLUIDYNE ENGINEERING CORPORATION

TABLE OF CONTENTS

	<u>Page</u>
DEFINITION OF SYMBOLS.	ii
LIST OF TABLES AND FIGURES	iv
INTRODUCTION	1
CONCLUSIONS.	2
DISCUSSION	3

TABLES

FIGURES

DATA SHEETS

DTIC QUALITY INSPECTED 3

Accession For	
NTIS	CRA&I
DTIC	TAB
Unannounced <input checked="" type="checkbox"/>	
Justification	
By	
Distribution/	
Availability Codes	
Dist	Avail and/or Special
A-1	

FLUIDYNE ENGINEERING CORPORATION

DEFINITION OF SYMBOLS

A	Local Area	square feet
A_e	Nozzle Exit Area	square feet
a	Local Speed of Sound	feet/second
C_D	Discharge Coefficient	
C_s	Stream Thrust Coefficient	
C_V	Thrust Coefficient Calculated Using p_s at Nozzle Exit	
F	Nozzle Exit Stream Thrust	pounds
G	Exhaust Thrust ($F - p_a A_e$)	pounds
M	Mach Number	
\dot{m}	Mass Flow	slugs/second
p_a	Static Pressure in Plenum Around Nozzle Exit	psfa
p_s	Static Pressure Inside Nozzle at the Exit	psfa
p_0	Total Pressure	psfa
p	Static Pressure	psfa
P_r	Prandtl Number	
R	Gas Constant for Air	53.35 feet/ $^{\circ}$ R
T	Static Temperature	$^{\circ}$ R
T_{aw}	Adiabatic Wall Temperature	$^{\circ}$ R
T_o	Total Temperature	$^{\circ}$ R
v	Velocity	feet/second
β	Ratio of Exit to Entrance Diameter of Nozzle	

FLUIDYNE ENGINEERING CORPORATION

γ Ratio of Specific Heats (C_p/C_v)
 λ Pressure Ratio (p_0/p_a)
 ρ Mass Density slugs/feet³

SUBSCRIPTS

act Actual
I Ideal Based on Ambient Conditions
i Ideal Based on Exit Static Conditions

FLUIDYNE ENGINEERING CORPORATION

LIST OF TABLES AND FIGURES

TABLE I. Tabulated Test Results

TABLE II. Dimensionless Static Pressure Distributions

<u>FIGURE</u>	<u>DESCRIPTION</u>
1.	ASME Flow Nozzle Installation
2.	Static Pressure Distributions
3.	Ratio of Nozzle Static to Ambient Pressure
4.	Ratio of Nozzle Static to Ambient Pressure - Expanded Scale
5.	Discharge Coefficient Versus Nozzle Pressure Ratio
6.	Discharge Coefficient Versus Throat Reynolds Number
7.	Thrust Coefficient Versus Nozzle Pressure Ratio
8.	Thrust Coefficient Versus Throat Reynolds Number
9-42.	Integrand Calculations and Plots

FLUIDYNE ENGINEERING CORPORATION

I. INTRODUCTION

This study, sponsored by the General Electric Company under their Purchase Order Number 200G230085, determined the discharge and velocity coefficients of an ASME long radius metering nozzle. Previous tests of this nozzle (Reference 1) had been conducted with an exhauster system which permitted operation at variable pressure ratio while keeping the Reynolds number constant. These additional tests were conducted to determine:

- A. Whether the presence of the exhauster duct or the survey rake significantly affected the integrated data.
- B. The effect of further changes of operating pressure ratio in the lower ranges of pressure ratio.
- C. The effect of decreasing the Reynolds number.

FLUIDYNE ENGINEERING CORPORATION

II. CONCLUSIONS

- A. These tests confirmed the observation made in the preceding test program (0431, Reference 1) that the core survey rake caused a consistent and appreciable increase in the measured static pressure, p_s , inside the nozzle near the exit. It may be concluded that this effect is present whether or not the exit plenum is installed. The effect is probably a manifestation of the sensitivity of transonic flow to small amounts of blockage, since the measured increase in pressure became greater as the pressure ratio approached the critical (choking) value.
- B. The nozzle discharge coefficient showed an increasing trend with Reynolds number, varying from 0.989 at $Re = 10^6$ to 0.992 at $Re = 10^7$. The nozzle pressure ratio showed no consistent, independent effect on the discharge coefficient.
- C. The nozzle thrust coefficient (at pressure ratios less than critical) also showed an increasing trend with Reynolds number, varying from 0.992 at $Re = 10^6$ to 0.995 at $Re = 6 \times 10^6$.

FLUIDYNE ENGINEERING CORPORATION

III. DISCUSSION

In the previous study conducted by FluiDyne, discharge and thrust coefficients were determined for a 7.715 inch diameter ASME long radius nozzle. The nozzle for these tests discharged into a cylindrical plenum in which pressure could be controlled by ejectors to vary the pressure ratio. The total pressure was held constant for most of the runs, giving a fairly constant throat Reynolds number.

For this test program, the metering nozzle discharged to atmosphere to eliminate any effects that might have been caused by the plenum on the first test series. Discharging to atmosphere meant that the nozzle pressure ratio and throat Reynolds number were controlled by the nozzle total pressure. Discharge and thrust coefficients were obtained over a pressure ratio range of 1.03 to 3.98 which corresponds to a Reynolds number variation of 0.95×10^6 to 12.0×10^6 .

The nozzle instrumentation was the same as for the previous test program except that the total pressure cross-rake, used to survey the core flow at the exit of the nozzle, was only installed on four runs. These four runs were made to determine the effect of the cross-rake on the static pressure near the nozzle exit. Mercury and water manometers were used for all pressure measurements.

The data reduction procedures used for these data were the same as described in the report for Project 0431. The calculations and plots of the integrands of the discharge and thrust coefficient equations are

FLUIDYNE ENGINEERING CORPORATION

shown in Figures 9 to 42. The tabulated test results are presented as Table I.

A plot of typical static pressure distributions through the nozzle is presented as Figure 2. A tabulation of these same typical static pressures is presented as Table II. The ratio of nozzle static to ambient pressure (P_s/P_a) is plotted versus nozzle pressure ratio for each data point of the two test programs and presented in Figure 3. Both sets of data closely follow the ideal curve for pressure ratios greater than two. For pressure ratios less than two, the data points taken on the 0431 program and the data points with the exit cross-rake installed on the 0470 program have a P_s/P_a ratio slightly higher than the ideal curve. The ratio of P_s/P_a in this lower pressure ratio range is presented as an expanded portion of the curve as Figure 4.

The nozzle discharge coefficients plotted versus nozzle pressure ratio and Reynolds number are presented as Figures 5 and 6, respectively. The discharge coefficients obtained in the previous study are also presented in these plots. The discharge coefficients obtained in the two test programs agree when compared on a throat Reynolds number basis, as would be expected from similitude considerations.

The two sets of thrust coefficient data, plotted versus nozzle pressure ratio, are presented as Figure 7. The same thrust coefficient data, obtained at pressure ratios equal to or less than two, are plotted

FLUIDYNE ENGINEERING CORPORATION

versus Reynolds number and presented as Figure 8. Good agreement is obtained between these two sets of data when compared at like pressure ratios. Good agreement is also obtained when compared on a Reynolds number basis.

Reference 1. "Determination of Discharge and Thrust Coefficients of a Choked ASME Nozzle from Exit Flow Surveys," James S. Holdhusen and Charles L. Landgraf, FluiDyne Project 0431, February 1965.

FLUIDYNE ENGINEERING CORPORATION

TABLE 1 TABULATED TEST RESULTS

Data Point	Press. Ratio	P_o (psia)	P_a (psia)	P_a / P_a	$\sqrt{\frac{P_a}{P_a} - \frac{T_1}{T}}$	$\int \left(\frac{M}{R} \right)^2 \frac{dA}{A}$	C_D	C_v	C_s	Thrust Re $\times 10^{-6}$
1	1.209	17.23	14.29	14.25	1.0031	.9902	.9927	1.1541	1.2689	2.47
2	2.403	35.20	18.21	14.25	1.2779	.9923	.9952	1.2248	1.2248	3.62
3	2.418	20.14	14.28	14.21	1.0052	.9905	.9953	1.2592	1.2592	4.66
4	1.643	23.34	14.32	14.21	1.0079	.9905	.9948	1.2683	1.2683	5.60
5	1.857	24.37	14.45	14.21	1.0176	.9915	.9952	1.2682	1.2682	6.19
6	2.059	29.25	15.41	14.21	1.0848	.9921	.9953	1.2704	1.2704	6.83
7	2.276	32.23	16.79	14.42	1.1860	.9924	.9968	1.2680	1.2680	7.47
8	2.487	35.21	18.35	14.42	1.2959	.9925	.9953	1.2683	1.2683	8.15
9	2.710	38.37	20.02	14.42	1.4141	.9925	.9941	1.2683	1.2683	8.70
10	2.904	41.05	21.27	14.14	1.5052	.9923	.9918	1.2688	1.2688	9.44
11	3.120	44.09	22.88	14.13	1.6193	.9925	.9925	1.2686	1.2686	10.0
12	3.355	47.20	24.57	14.05	1.7491	.9925	.9883	1.2678	1.2678	10.6
13	3.568	50.10	26.11	14.04	1.8602	.9924	.9880	1.2681	1.2681	11.2
14	3.773	52.96	27.60	14.04	1.9662	.9926	.9880	1.2683	1.2683	12.0
15	3.985	55.93	29.27	14.03	2.0854	.9930	.9885	1.2683	1.2683	12.9
16*	3.929	55.13	28.79	14.03	2.0513	.9924	.9878	1.2683	1.2683	12.52
17	4.219	17.12	14.07	14.04	1.0021	.9903	.9836	1.2681	1.2681	3.62
18	4.431	20.09	14.10	14.04	1.0045	.9911	.9853	1.2683	1.2683	4.60
19	4.647	23.13	14.13	14.04	1.0066	.9912	.9855	1.2683	1.2683	5.17
20	4.613	23.14	14.13	14.04	1.0063	.9903	.9840	1.2683	1.2683	5.54
21	4.859	26.10	14.28	14.04	1.0171	.9917	.9870	1.2683	1.2683	6.17
22	5.066	29.00	15.25	14.04	1.0861	.9922	.9876	1.2711	1.2711	6.17
23	5.073	29.11	15.27	14.04	1.0875	.9923	.9876	1.2711	1.2711	6.17
24	5.213	17.10	14.14	14.09	1.0035	.9908	.9843	1.2684	1.2684	2.53
25	5.1647	23.21	14.48	14.09	1.0278	.9918	.9864	1.2681	1.2681	4.62
26	5.498	35.20	18.85	14.09	1.3373	.9928	.9879	1.2683	1.2683	7.49
27	5.488	35.07	18.81	14.09	1.3348	.9925	.9878	1.2683	1.2683	7.43
28	5.128	44.13	22.94	14.11	1.6260	.9927	.9882	1.2683	1.2683	4.51
29	5.136	44.24	23.02	14.11	1.6319	.9928	.9882	1.2683	1.2683	4.60
2-1	1.032	14.05	14.28	14.27	1.00007	.9893	.9815	1.0402	1.0402	0.94
2-2	1.053	14.930	14.229	14.27	1.000010	.9900	.9818	1.0571	1.0571	1.25
2-3	1.106	15.738	14.229	14.27	1.000012	.9898	.9818	1.0968	1.0968	1.73
2-4	1.152	16.397	14.231	14.27	1.000027	.9897	.9827	1.1261	1.1261	2.11
2-5	1.202	17.099	14.232	14.27	1.000033	.9900	.9835	1.1523	1.1523	2.42

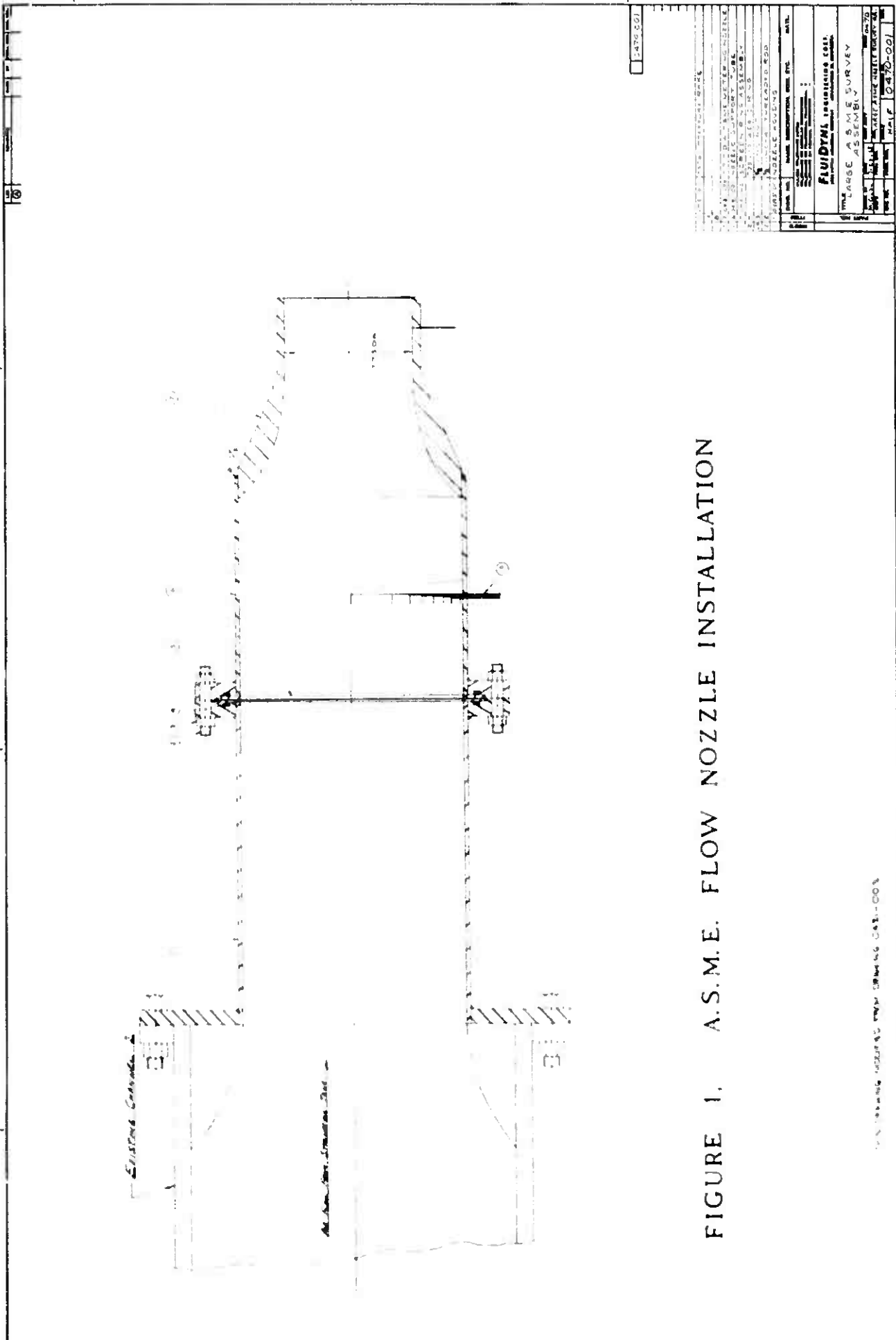
FLUIDYNE ENGINEERING CORPORATION

TABLE II
DIMENSIONLESS STATIC PRESSURE DISTRIBUTIONS
(P/P_o)

Run Number	$\frac{P_o}{P_a}$	$\frac{P_o}{\lambda}$	Values of P/P_o								
			1-4*	5	6	7	8	9	10	11	12
1	1.209	.8271	.8295	.8310	.8324	.8310	.8239	.8197	.8182	.8011	.8410
3	1.418	.7052	.7088	.7125	.7161	.7125	.7003	.6930	.6930	.7015	.7477
4	1.643	.6086	.6135	.6169	.6232	.6211	.6065	.5971	.5950	.6191	.6943
5	1.857	.5385	.5481	.5609	.5702	.5729	.5609	.5488	.5479	.5896	.6787
6	2.059	.4857	.5269	.5477	.5611	.5661	.5544	.5419	.5419	.5879	.6791
8	2.276	.4394	.5212	.5473	.5587	.5632	.5518	.5397	.5397	.5860	.6764
9	2.487	.4021	.5211	.5453	.5599	.5641	.5522	.5404	.5404	.5863	.6780
11	2.904	.3444	.5184	.5441	.5572	.5626	.5501	.5382	.5382	.5853	.6783
14	3.568	.2803	.5213	.5445	.5582	.5636	.5504	.5387	.5387	.5856	.6774
16b	3.929	.2545	.5222	.5453	.5591	.5640	.5502	.5391	.5391	.5857	.6794

*Average

FLUIDYNE ENGINEERING CORPORATION



FLUIDYNE ENGINEERING CORPORATION

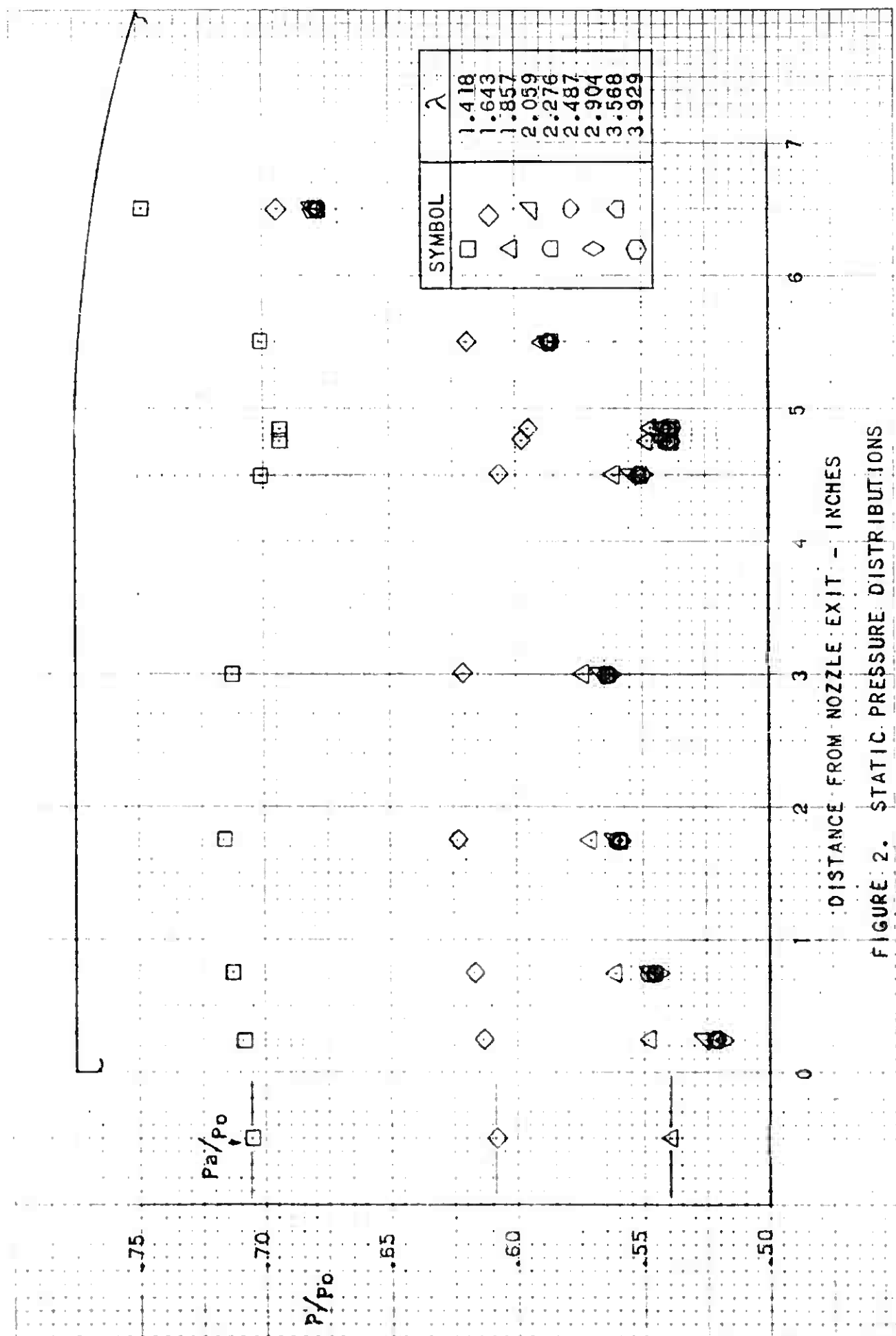
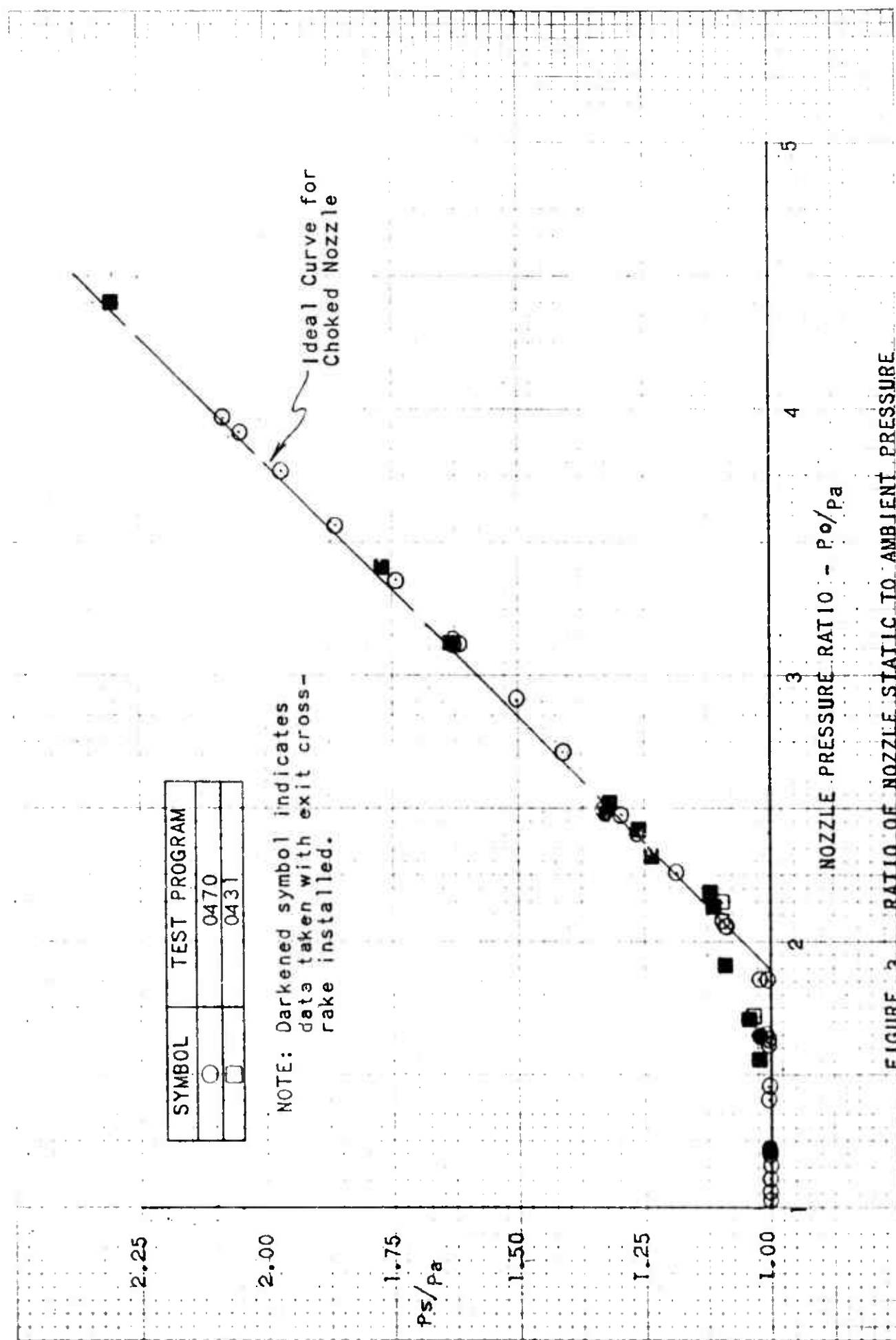


FIGURE 2. STATIC PRESSURE DISTRIBUTIONS

FLUIDYNE ENGINEERING CORPORATION



FLUIDYNE ENGINEERING CORPORATION

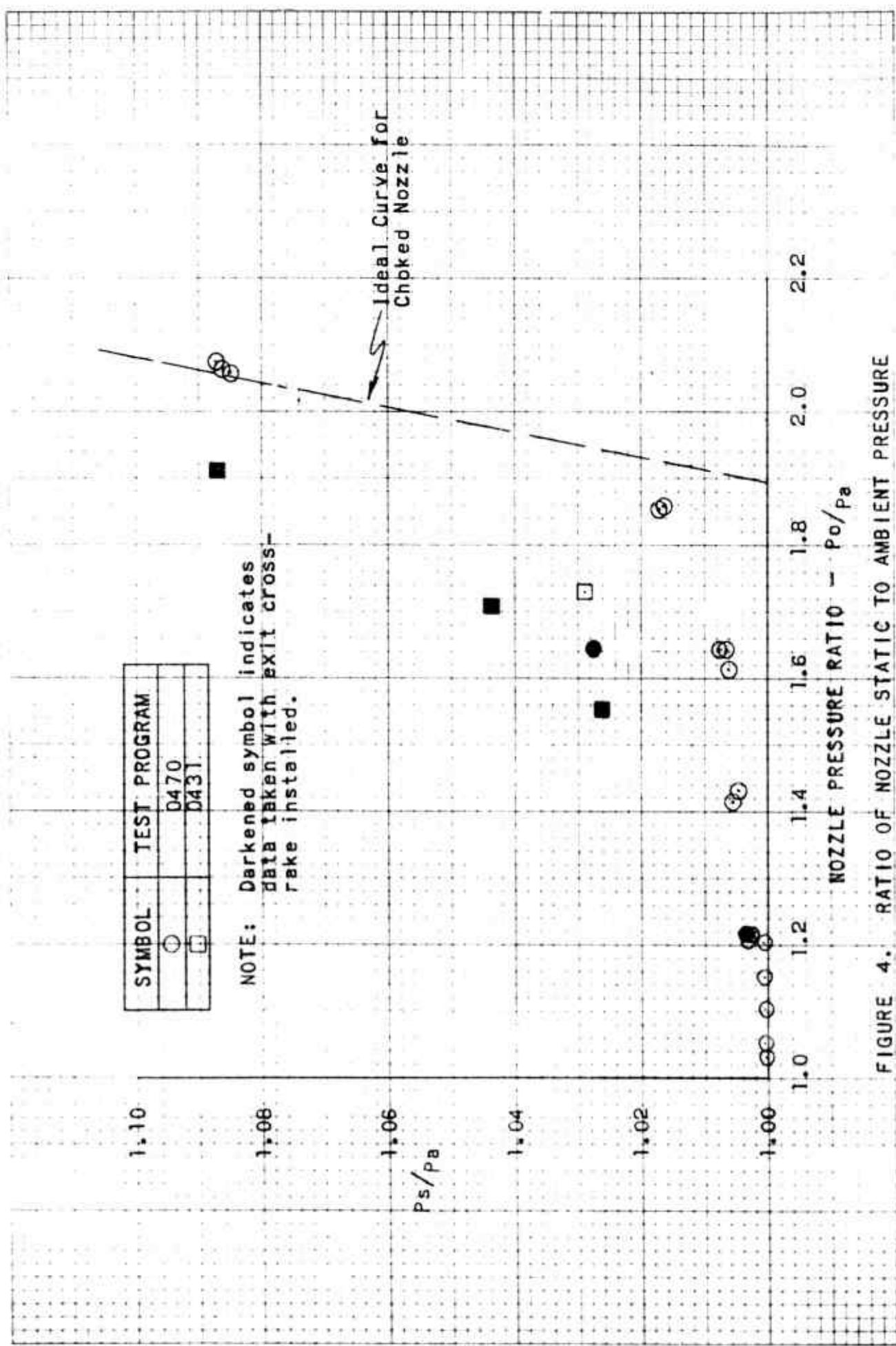


FIGURE 4. RATIO OF NOZZLE STATIC TO AMBIENT PRESSURE

NO 3400-110 DIETZGEN GRAPHIC PAPER
1 CYCLE X 10 DIVISIONS PER INCH

EUGENE DIETZGEN CO.
MADE IN U.S.A.

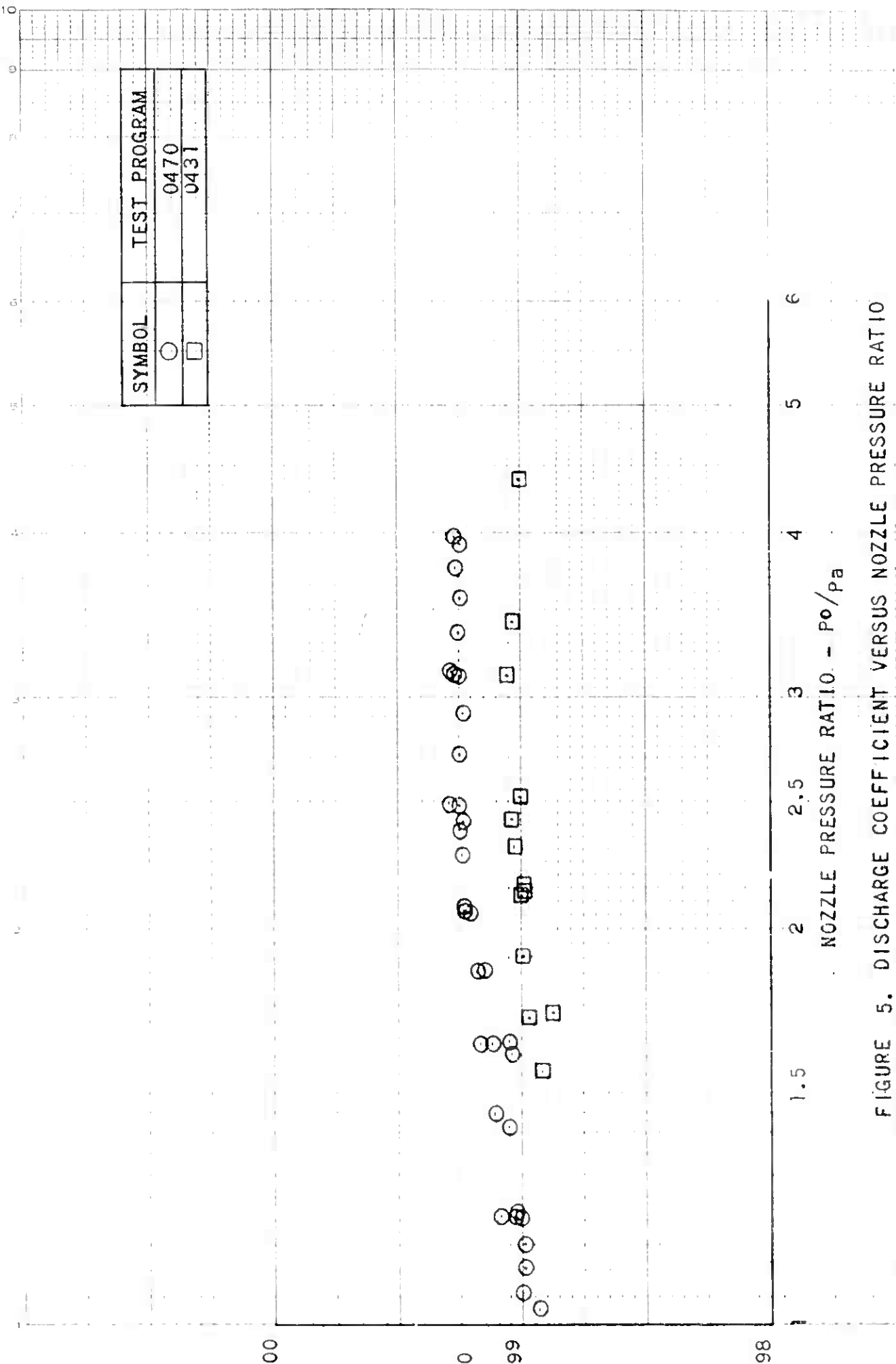


FIGURE 5. DISCHARGE COEFFICIENT VERSUS NOZZLE PRESSURE RATIO

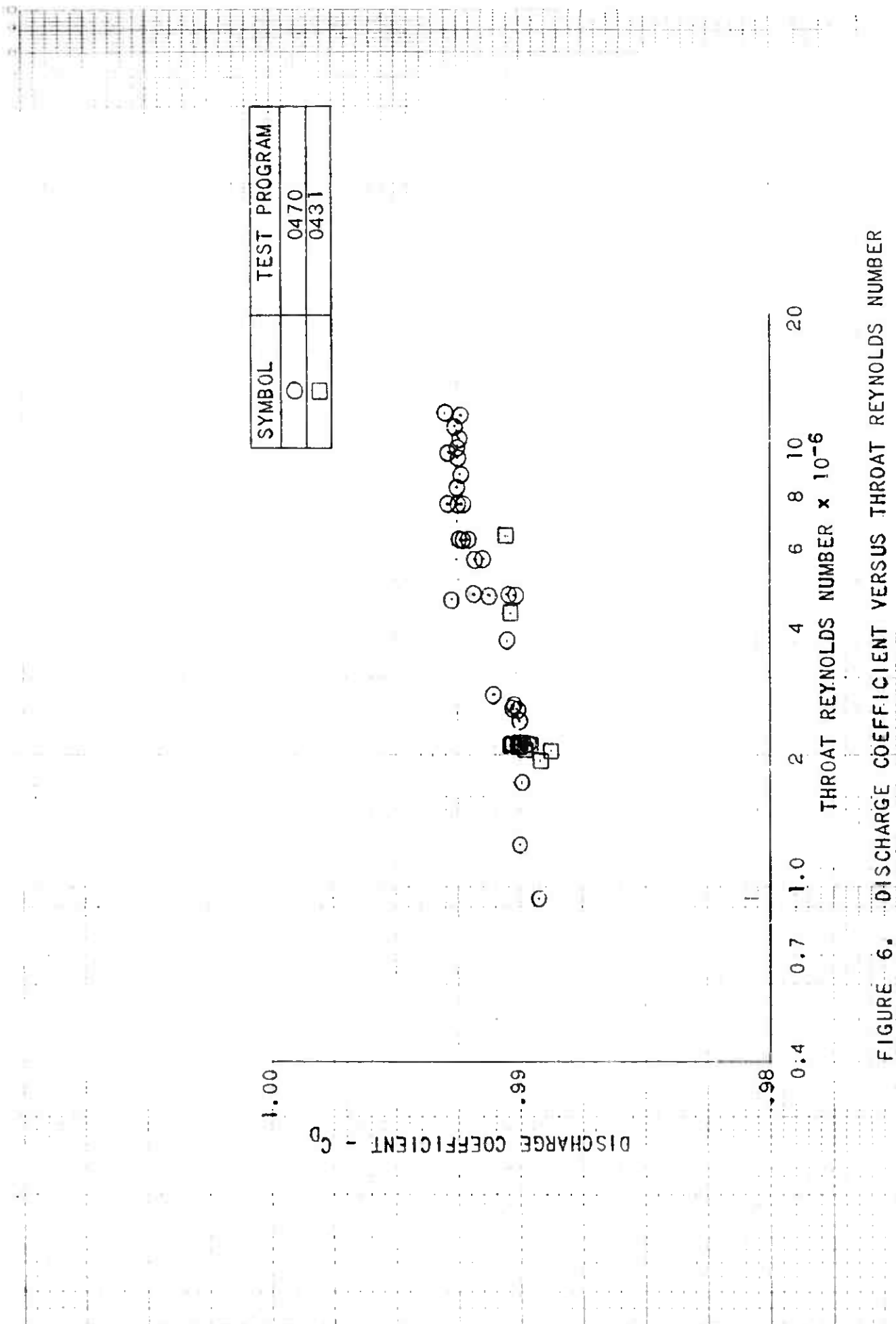


FIGURE 6. DISCHARGE COEFFICIENT VERSUS THROAT REYNOLDS NUMBER

NO. 3400-1110 DIETZGEN GRAPH PAPER
51 MI-LOGARITHMIC
1 CYCLIX 10 DIVISIONS PER INCH

EUGENE DIETZGEN CO.
MADE IN U. S. A.

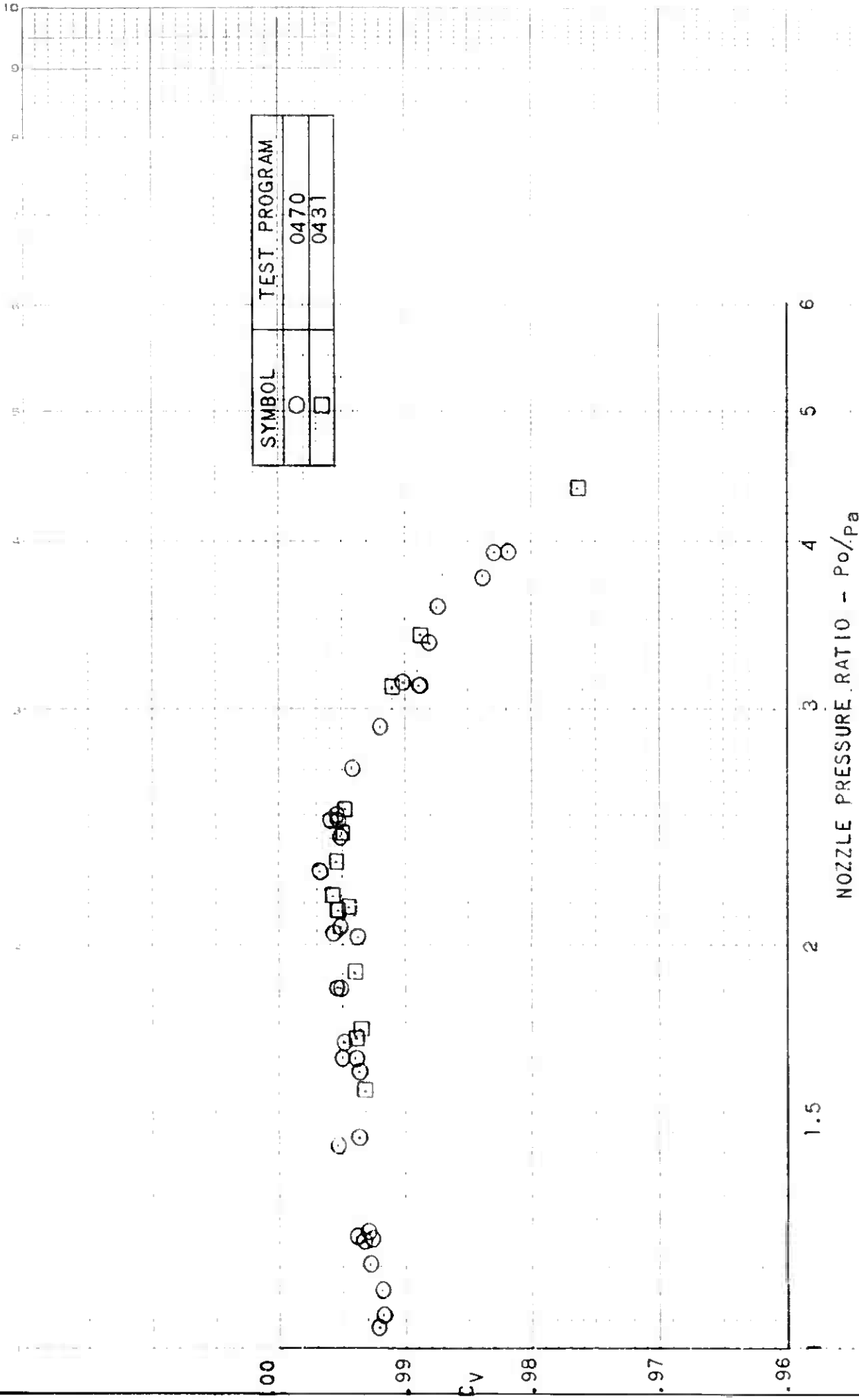


FIGURE 7. THRUST COEFFICIENT VERSUS NOZZLE PRESSURE RATIO

TEST PROGRAM	
SYMBOL	
○	0470
□	0431

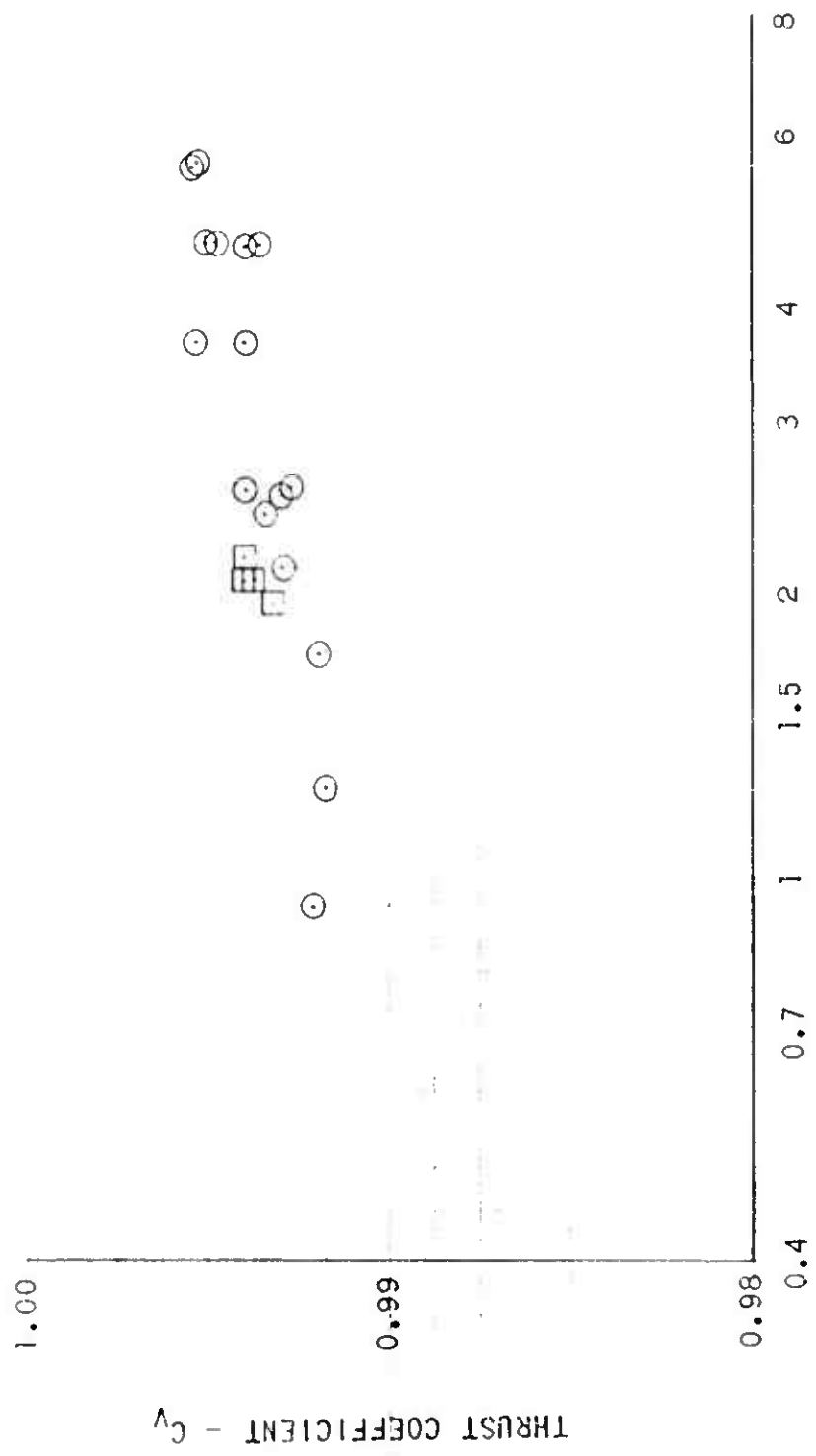
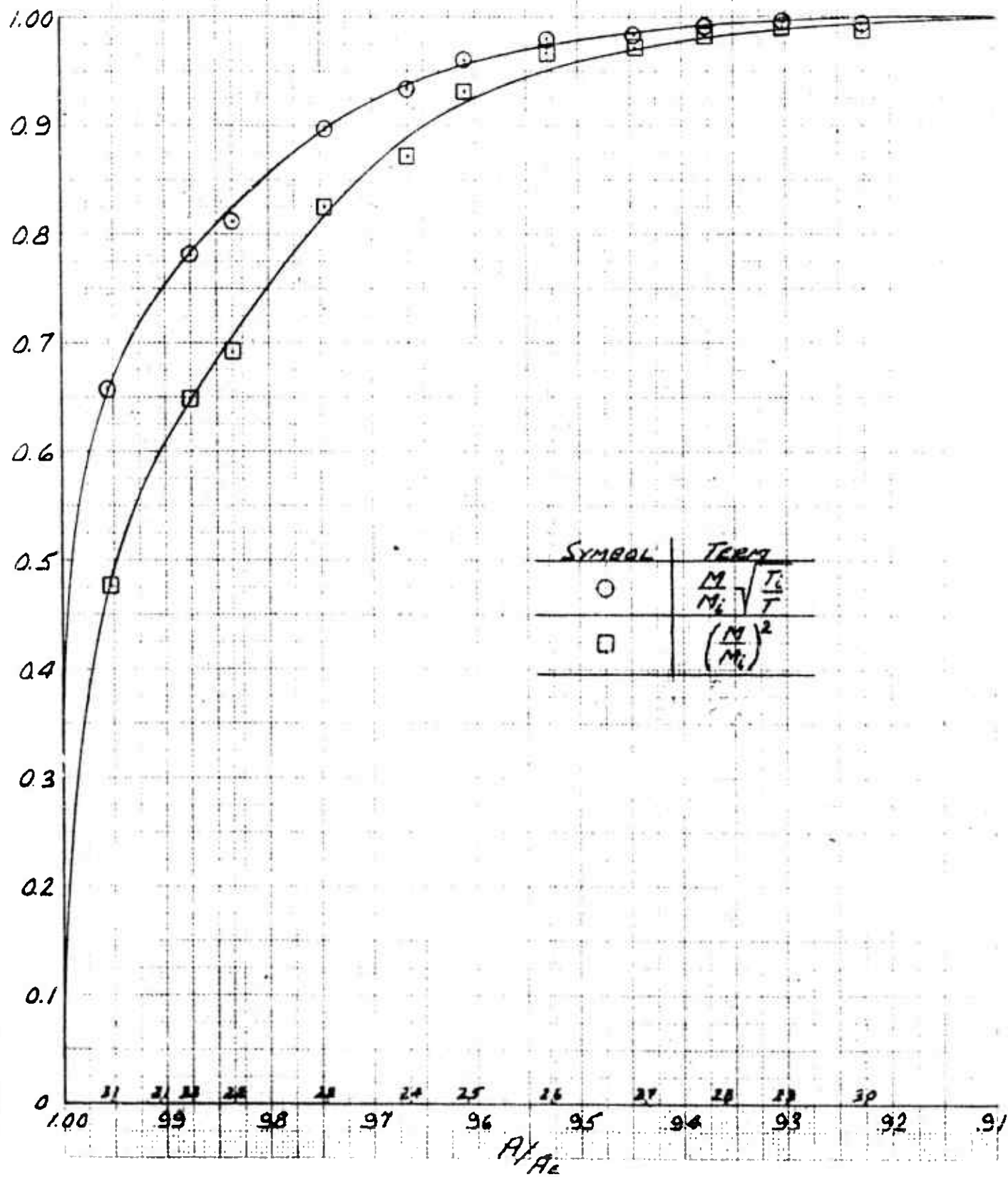


FIGURE 8. THRUST COEFFICIENT VERSUS THROAT REYNOLDS NUMBER

FLUIDYNE ENGINEERING CORPORATION

INTEGRATION CURVES
TO DETERMINE C_d & C_v

RUN - 2 DATA POINT 2.4706

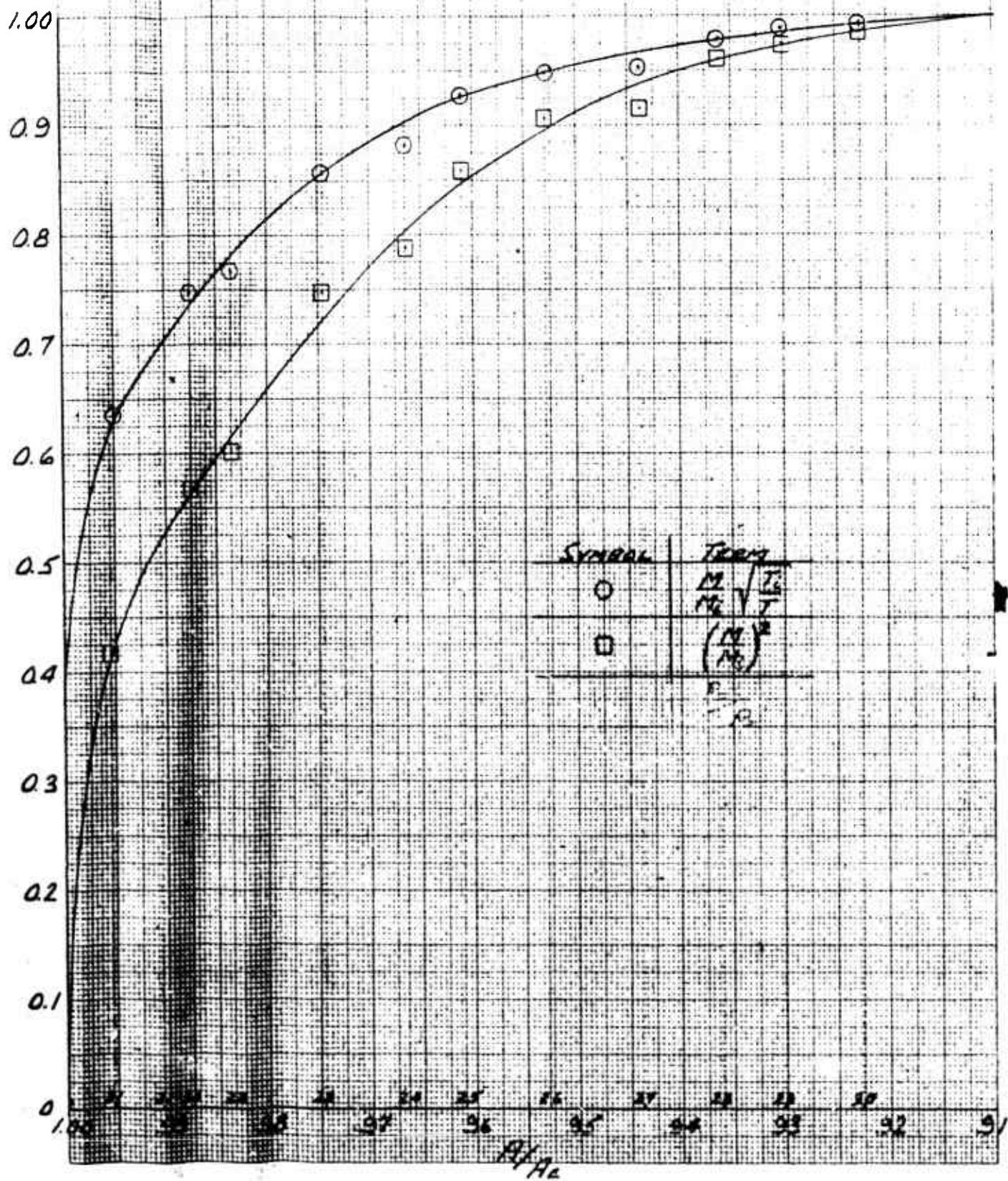


FLUIDYNE ENGINEERING CORPORATION

INTEGRATION CURVES

TO DETERMINE C_D & C_V

RUN 1 DATA POINT 1.2092



FLUIDYNE ENGINEERING CORPORATION

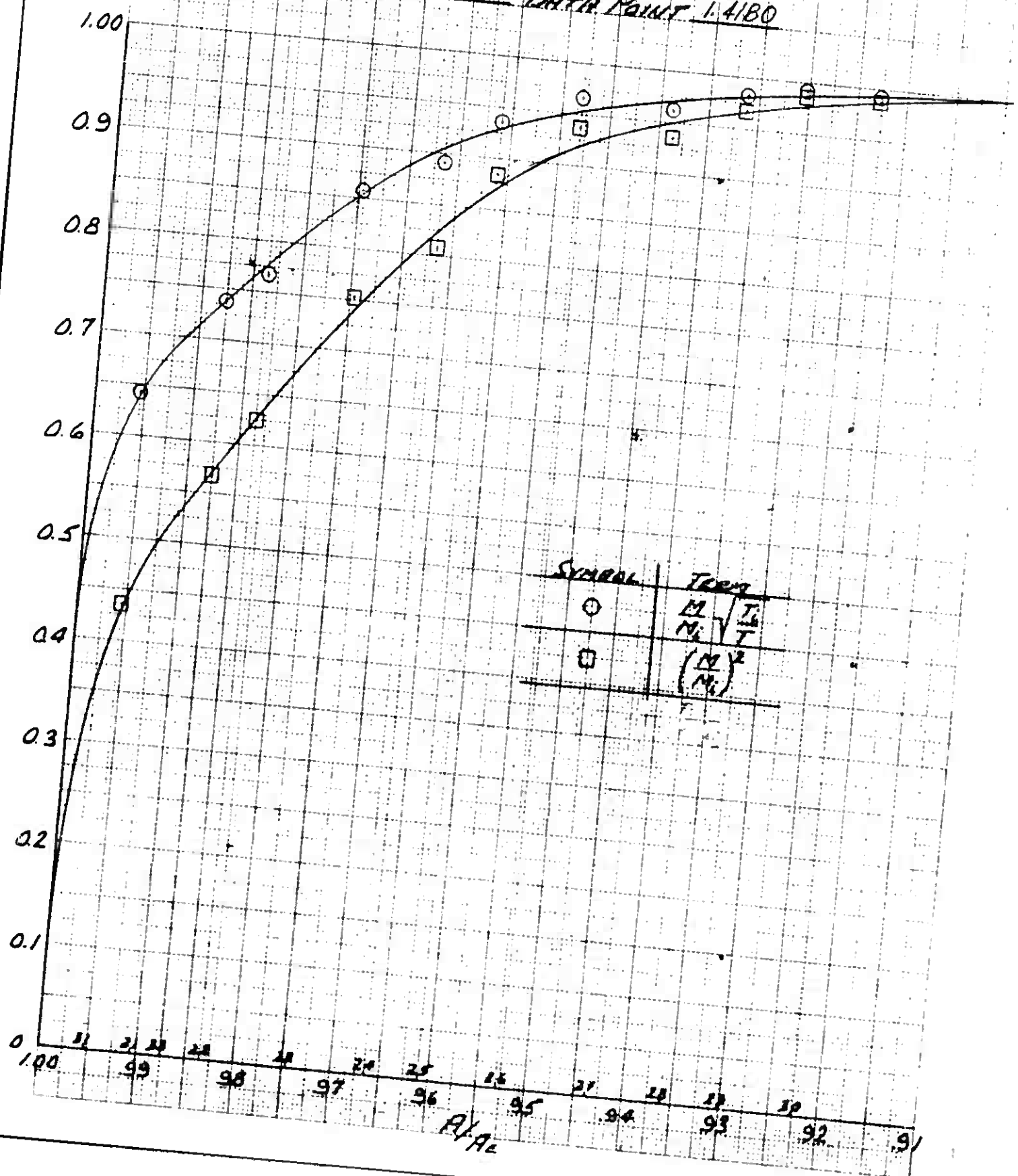
0786
5066

INTEGRATION CURVES

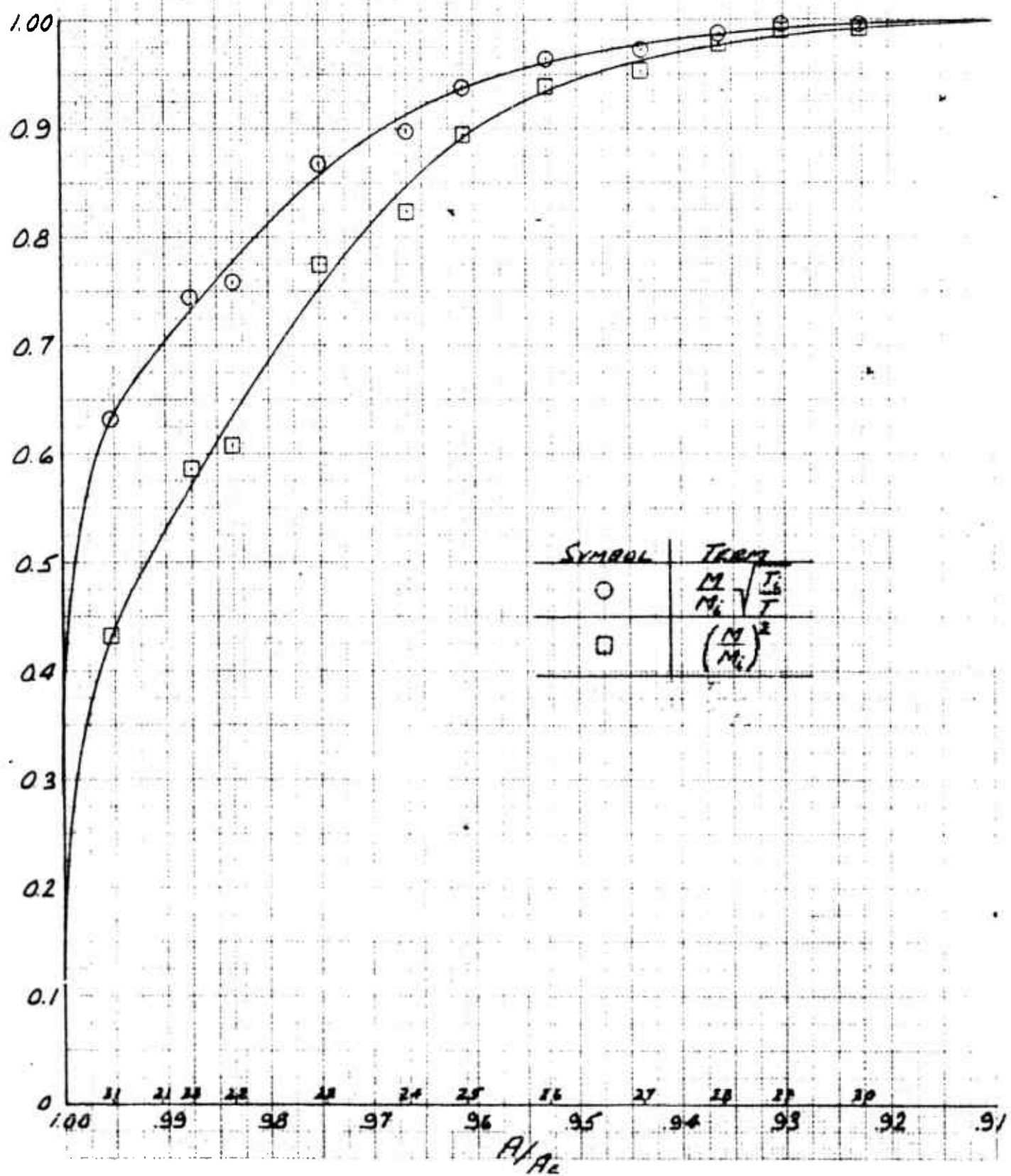
To DETERMINE C_0 & C_1

Run 3

DATA POINT 1.4180



FLUIDYNE ENGINEERING CORPORATION

1536
50hbINTEGRATION CURVESTO DETERMINE C_D & C_V RUN 4 DATA POINT 1.6430

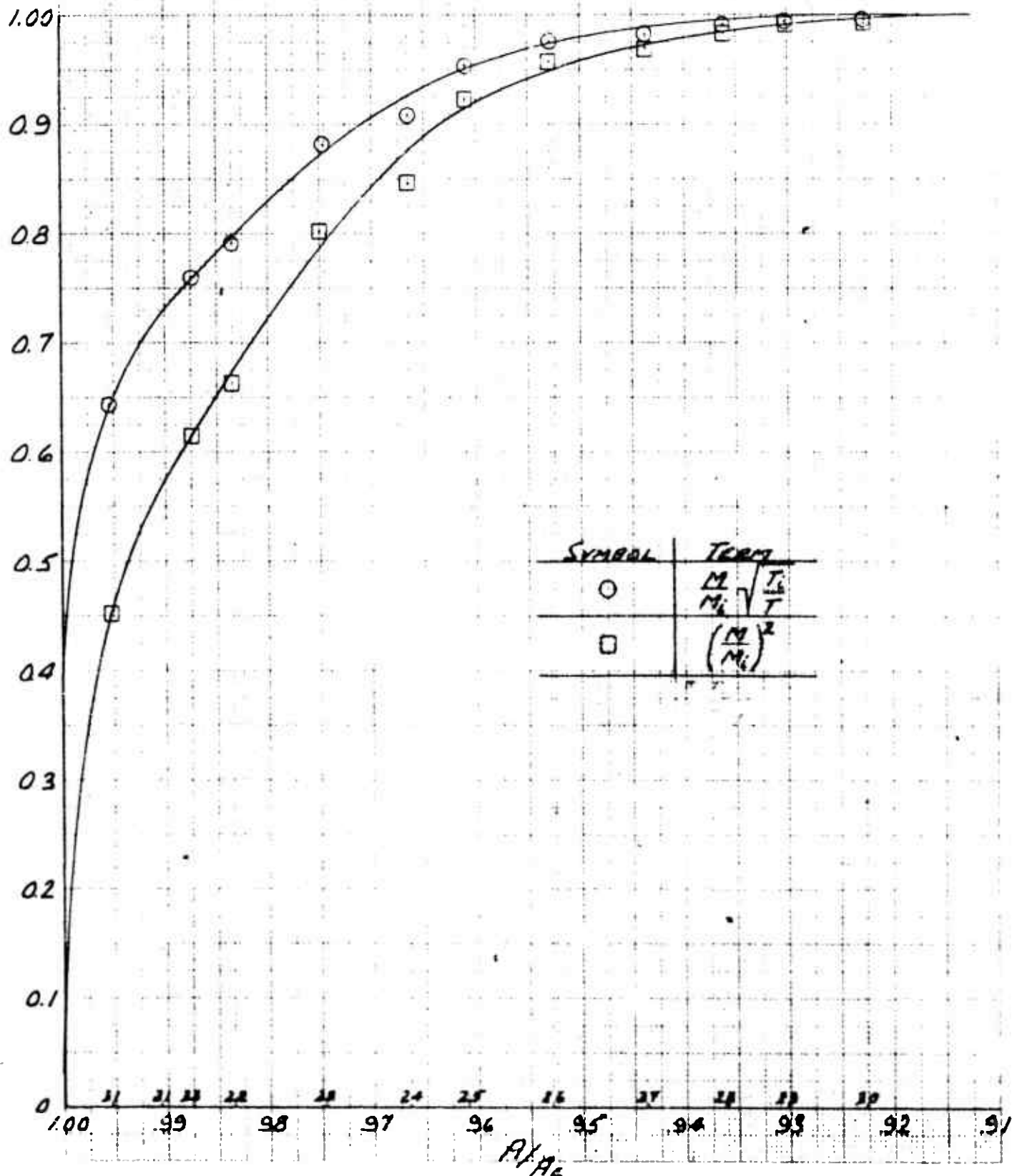
FLUIDYNE ENGINEERING CORPORATION

593 b
5166

INTEGRATION CURVES

To DETERMINE C_d & C_v

RUN - 5 DATA POINT 1.8567



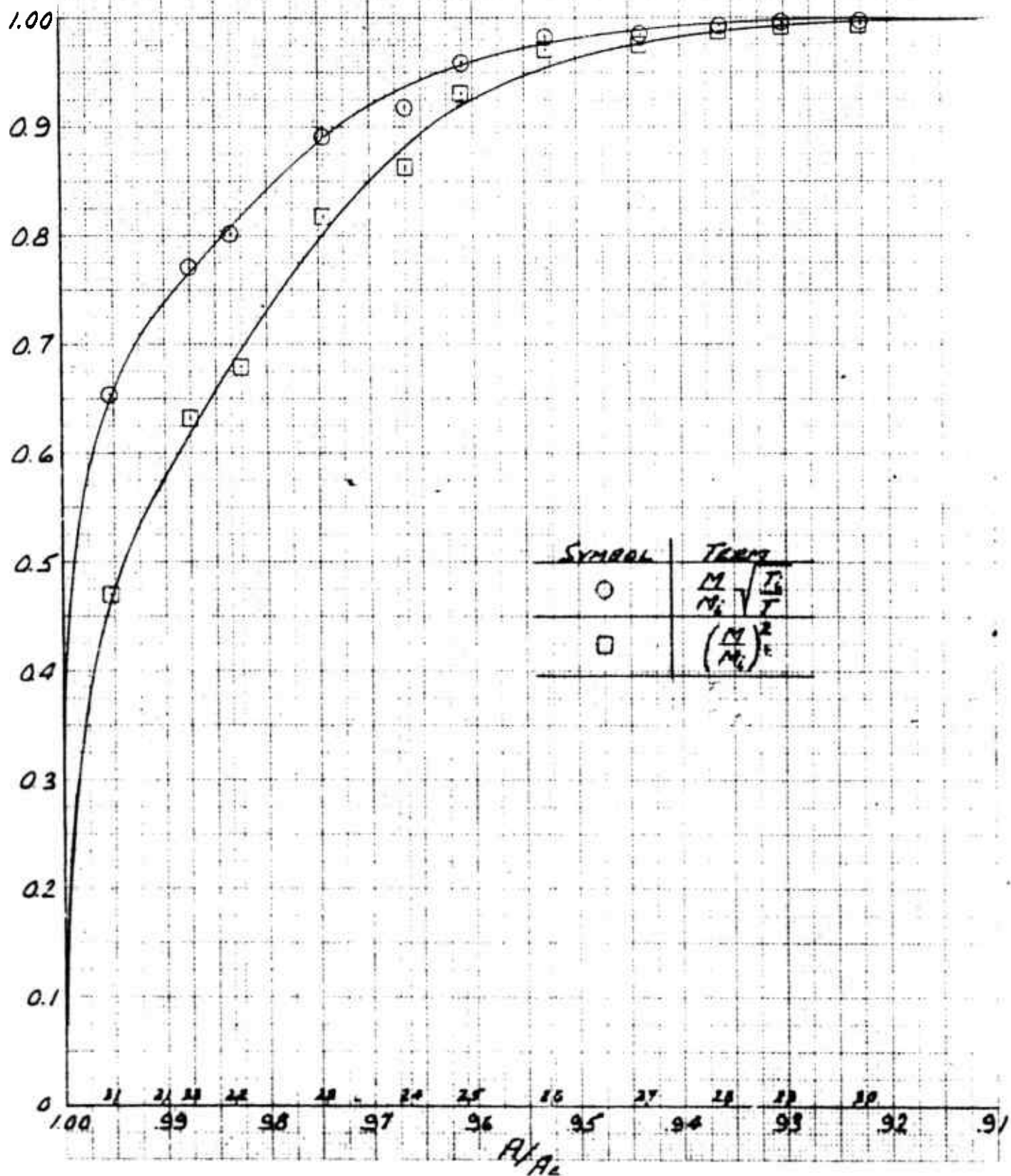
FLUIDYNE ENGINEERING CORPORATION

b98b
lebb

INTEGRATION CURVES

TO DETERMINE C_d & C_v

RUN 6 DATA POINT 2.0589

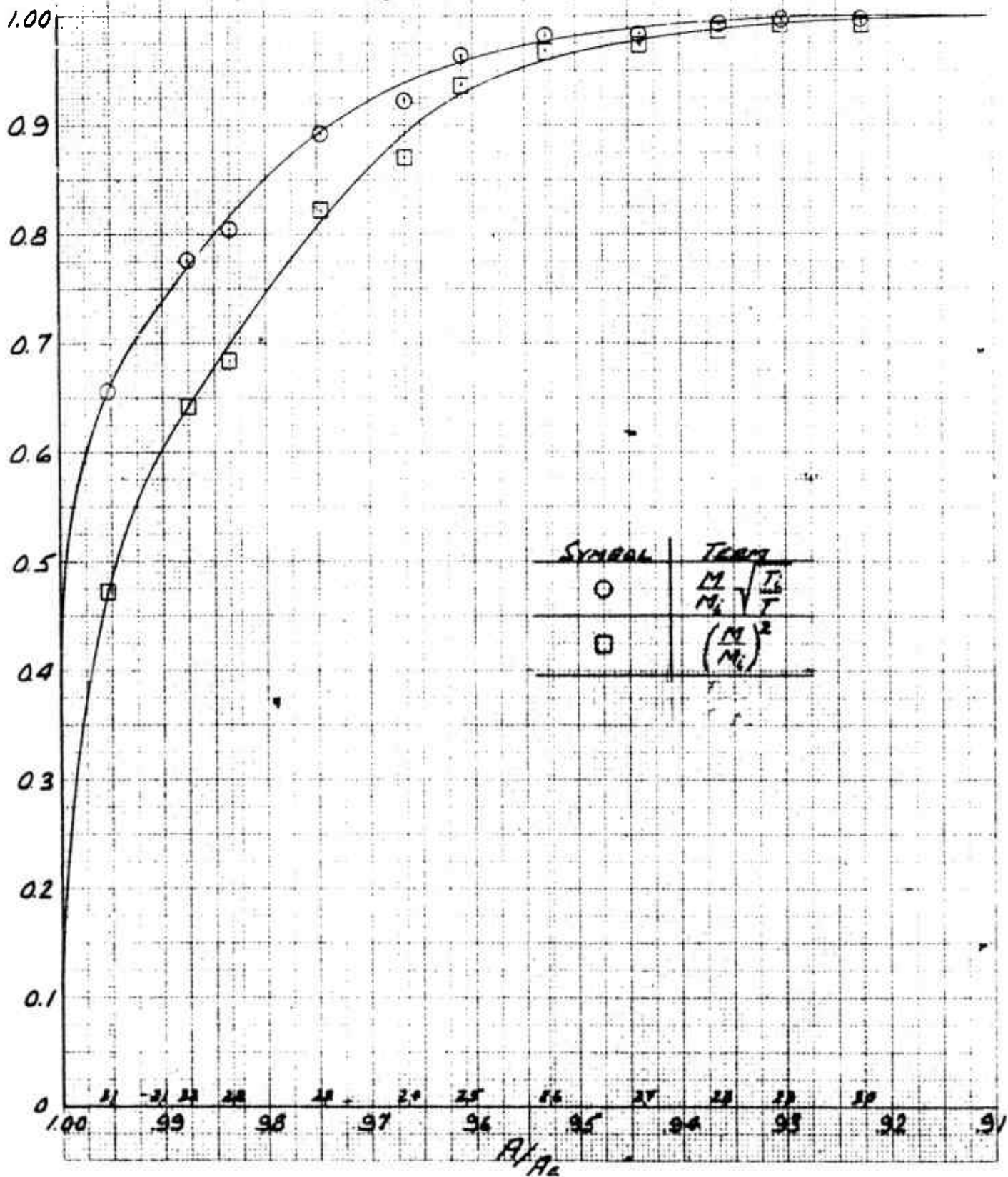


FLUIDYNE ENGINEERING CORPORATION

1685
1266

INTEGRATION CURVES
TO DETERMINE C_D & C_V

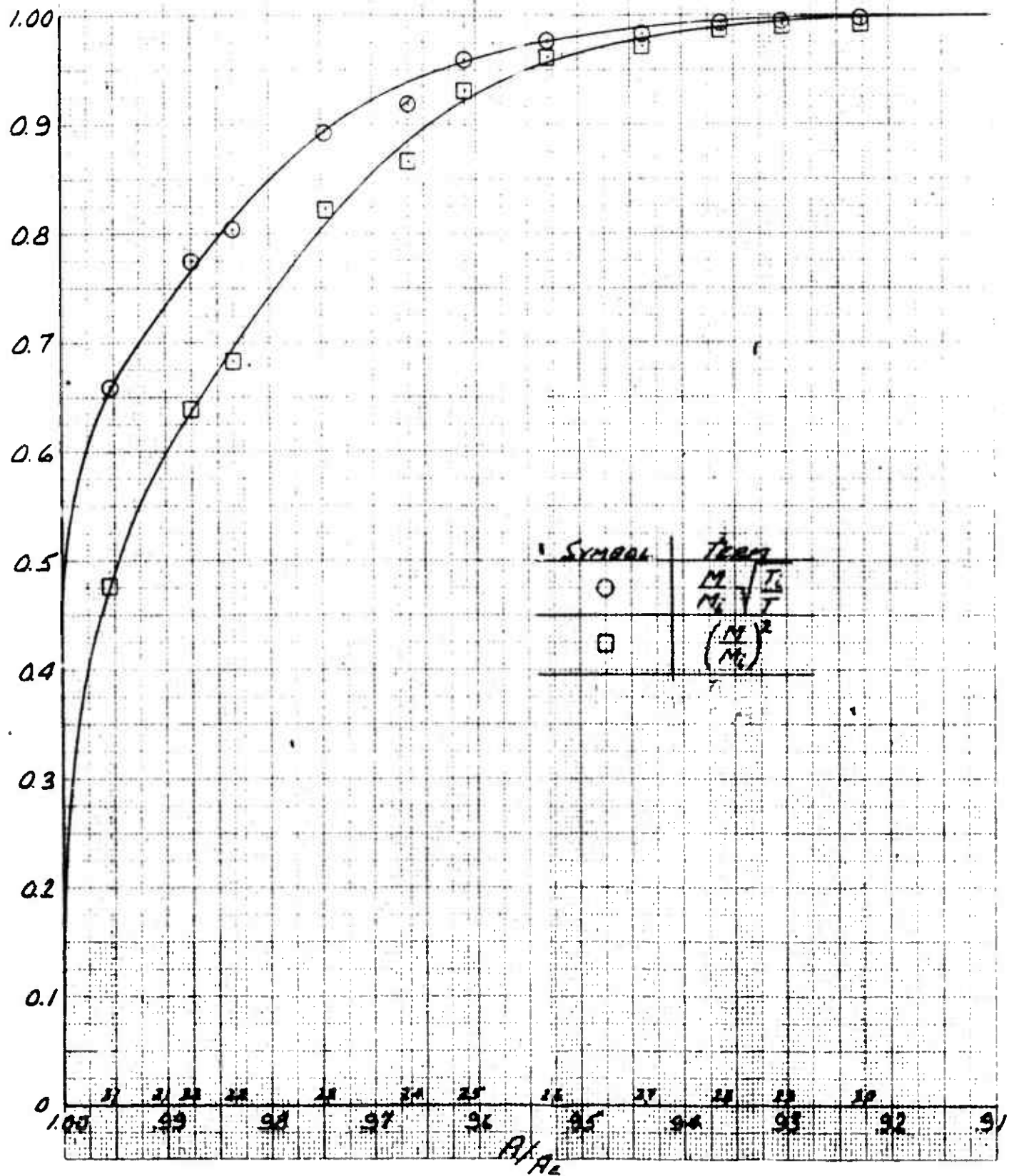
RUN - 7 DATA POINT 2,2547



FLUIDYNE ENGINEERING CORPORATION

643
1266INTEGRATION CURVESTO DETERMINE C_d & C_v

RUN 8 DATA POINT 2.2762

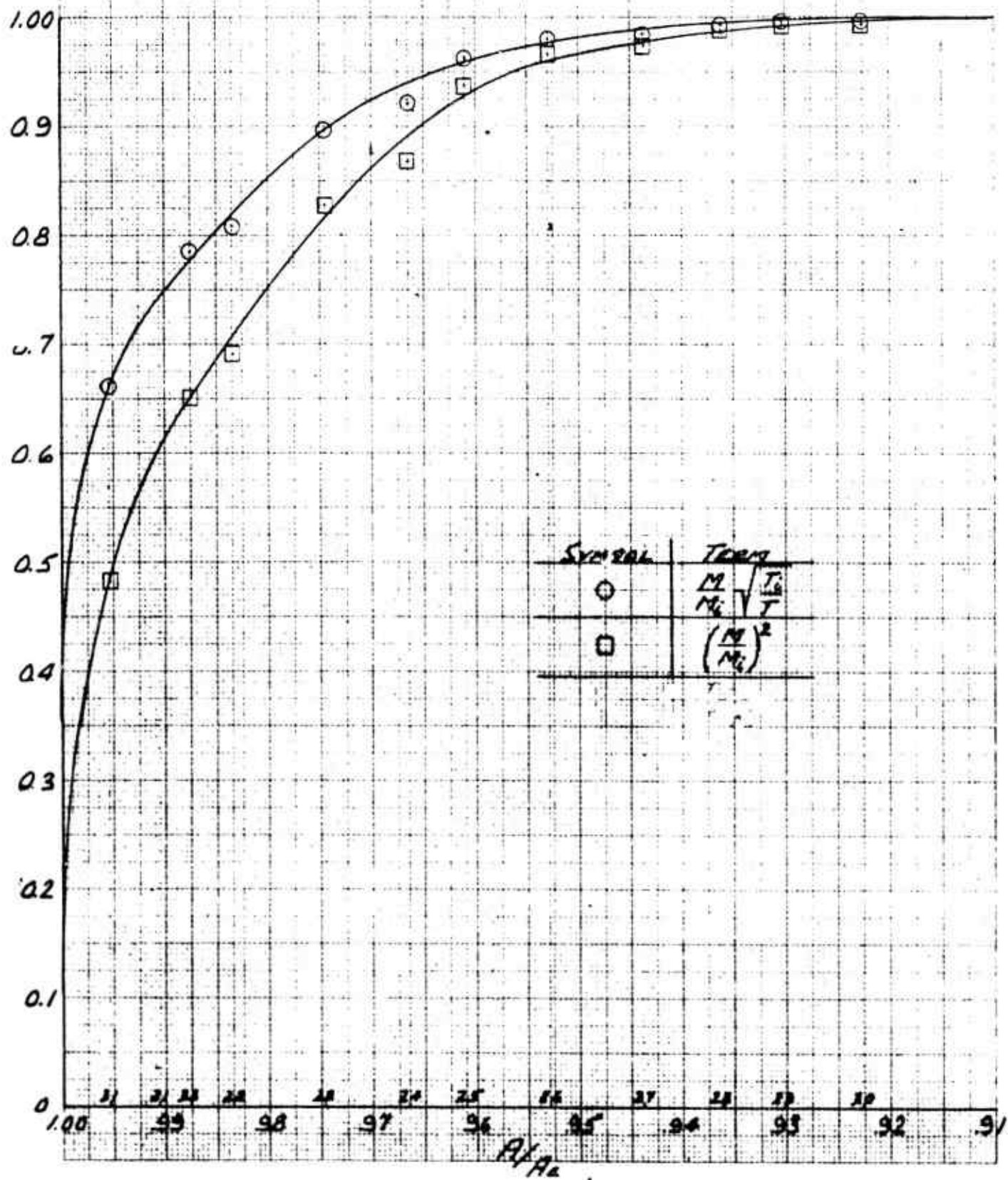


Symbol	Term
○	$\frac{M}{M_1} \sqrt{\frac{T_1}{T}}$
□	$\left(\frac{M}{M_1}\right)^2$

FLUIDYNE ENGINEERING CORPORATION

836
566INTEGRATION CURVES
TO DETERMINE C_D & C_V

RUN 9 DATA POINT 24867



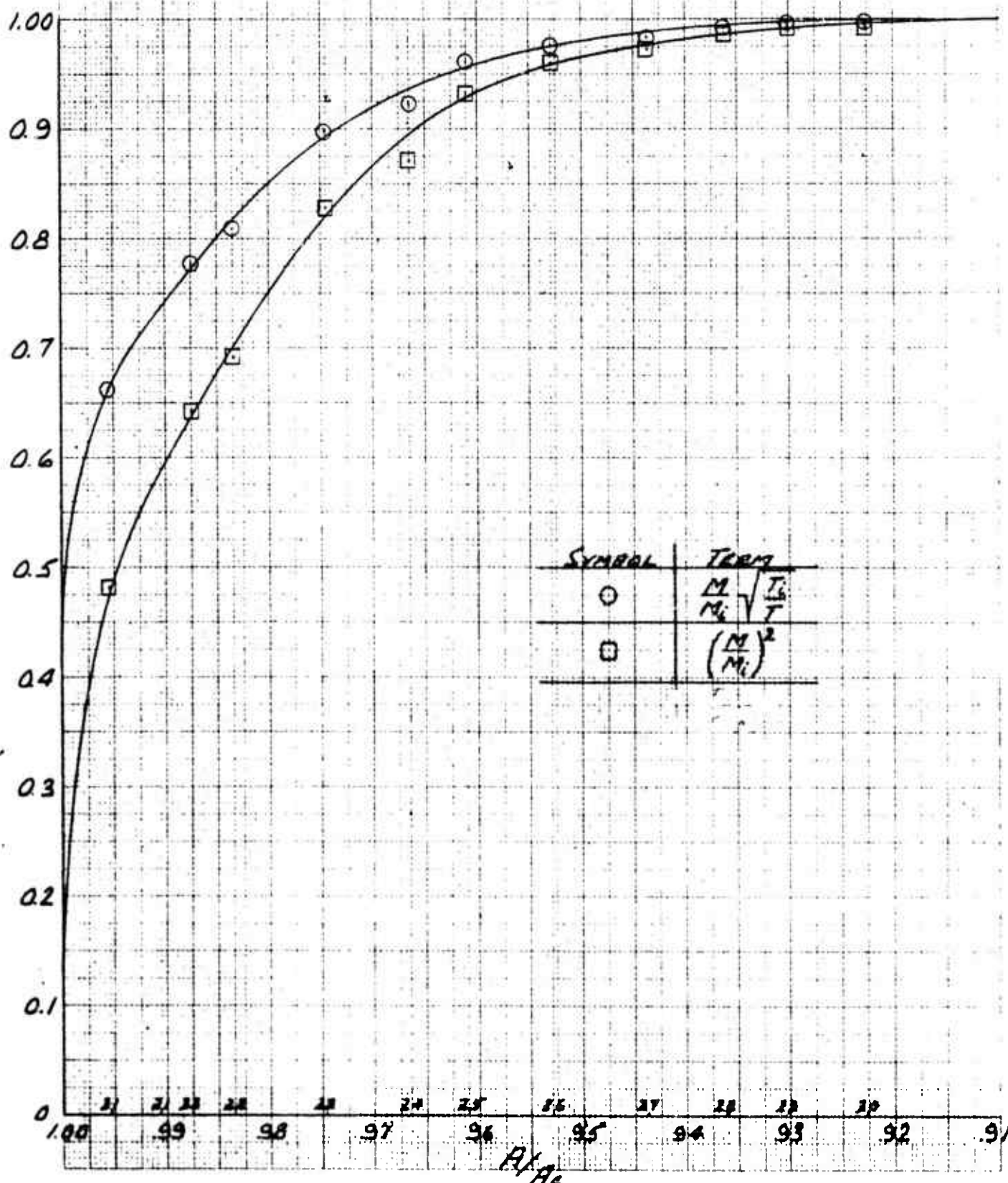
FLUIDYNE ENGINEERING CORPORATION

9136
5/66

INTEGRATION CURVES

TO DETERMINE C_0 & C_V

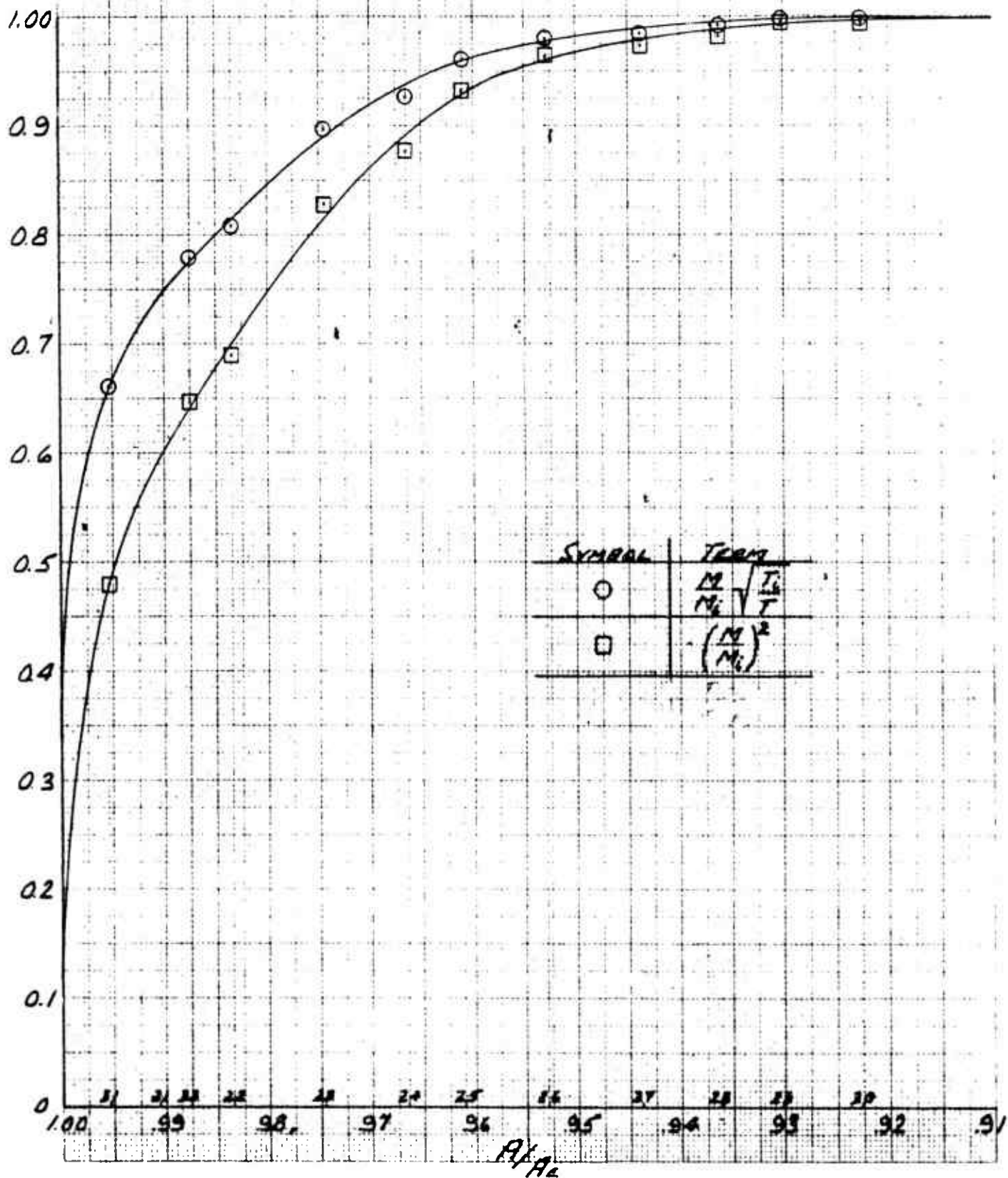
RUN 10 DATA POINT 2.7096



FLUIDYNE ENGINEERING CORPORATION

INTEGRATION CURVES
TO DETERMINE C_D & C_V

RUN 11 DATA POINT 2.9037



FLUIDYNE ENGINEERING CORPORATION

0381
gtbb

INTEGRATION CURVES

TO DETERMINE C_D & C_V :

RUN 12 DATA POINT 3/120

1.00

0.9

0.8

0.7

0.6

0.5

0.4

0.3

0.2

0.1

0

Symbol	Term
$M_1 \frac{V_1}{A_1}$	$\frac{C_D}{C_V} V^2$
$(\frac{A_1}{A_2})^2$	

A_1/A_2

0.00 0.05 0.10 0.15 0.20 0.25 0.30 0.35 0.40 0.45 0.50 0.55 0.60 0.65 0.70

0.75

5166
5166

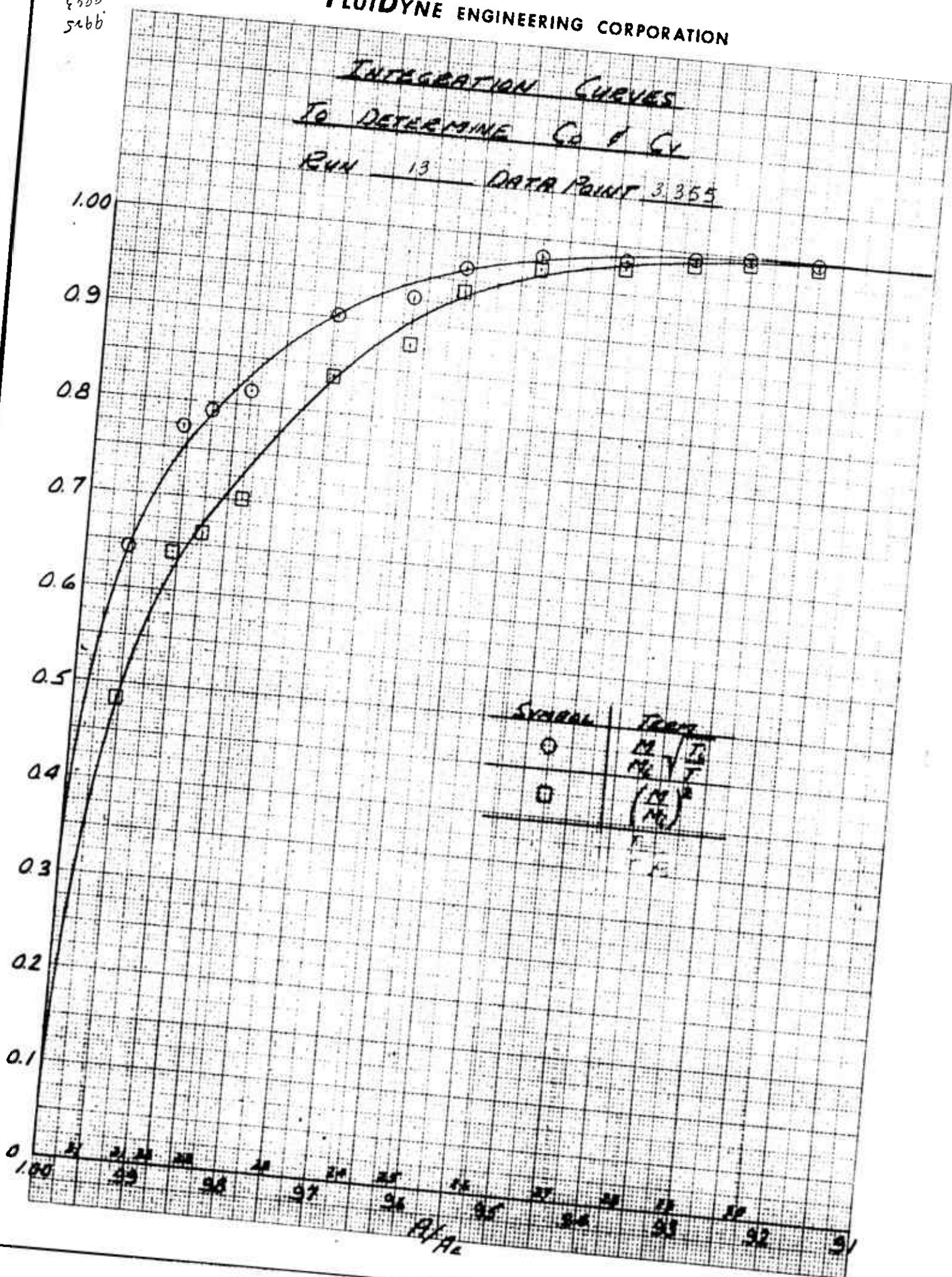
FLUIDYNE ENGINEERING CORPORATION

INTEGRATION CURVES

To DETERMINE C_d & C_v

Run 13

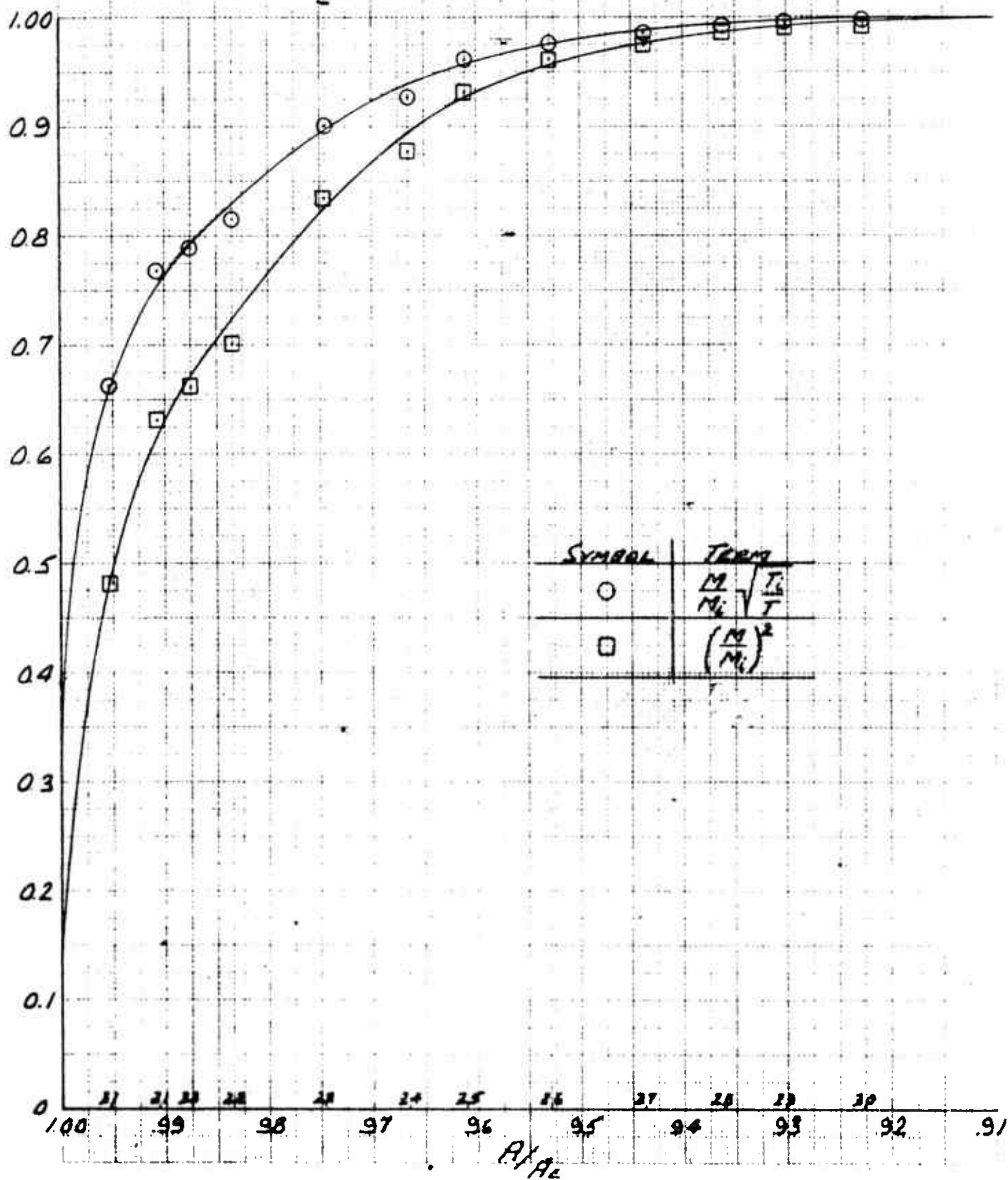
DATA POINTS 31355



FLUIDYNE ENGINEERING CORPORATION

0836
nebbINTEGRATION CURVESTO DETERMINE C_d & C_v

RUN 14 DATA POINT 3.568

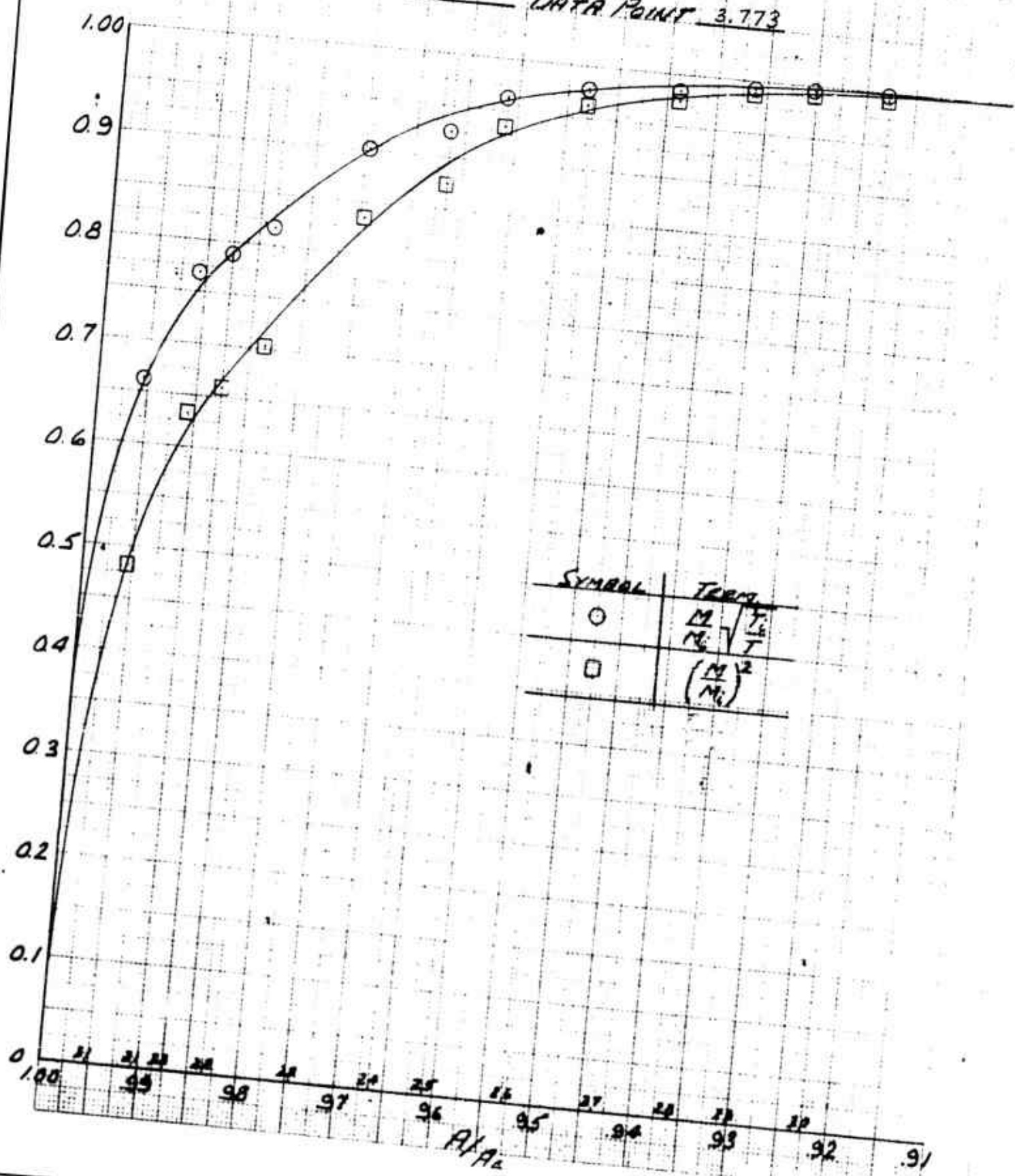


FLUIDYNE ENGINEERING CORPORATION

0336
9266

INTEGRATION CURVES
TO DETERMINE C_D & C_V

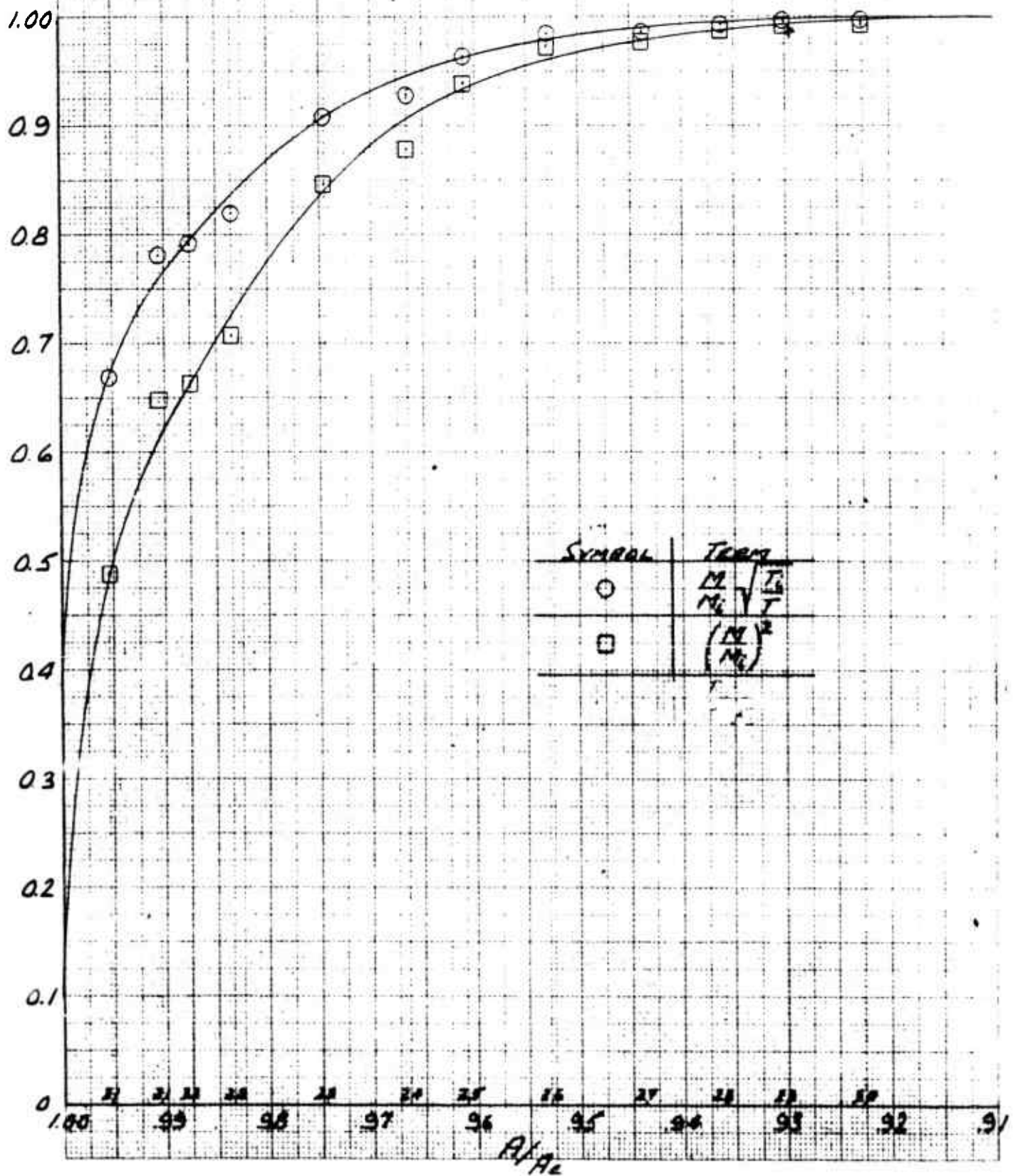
RUN 15 DATA POINT 3.773



FLUIDYNE ENGINEERING CORPORATION

3236
08bb

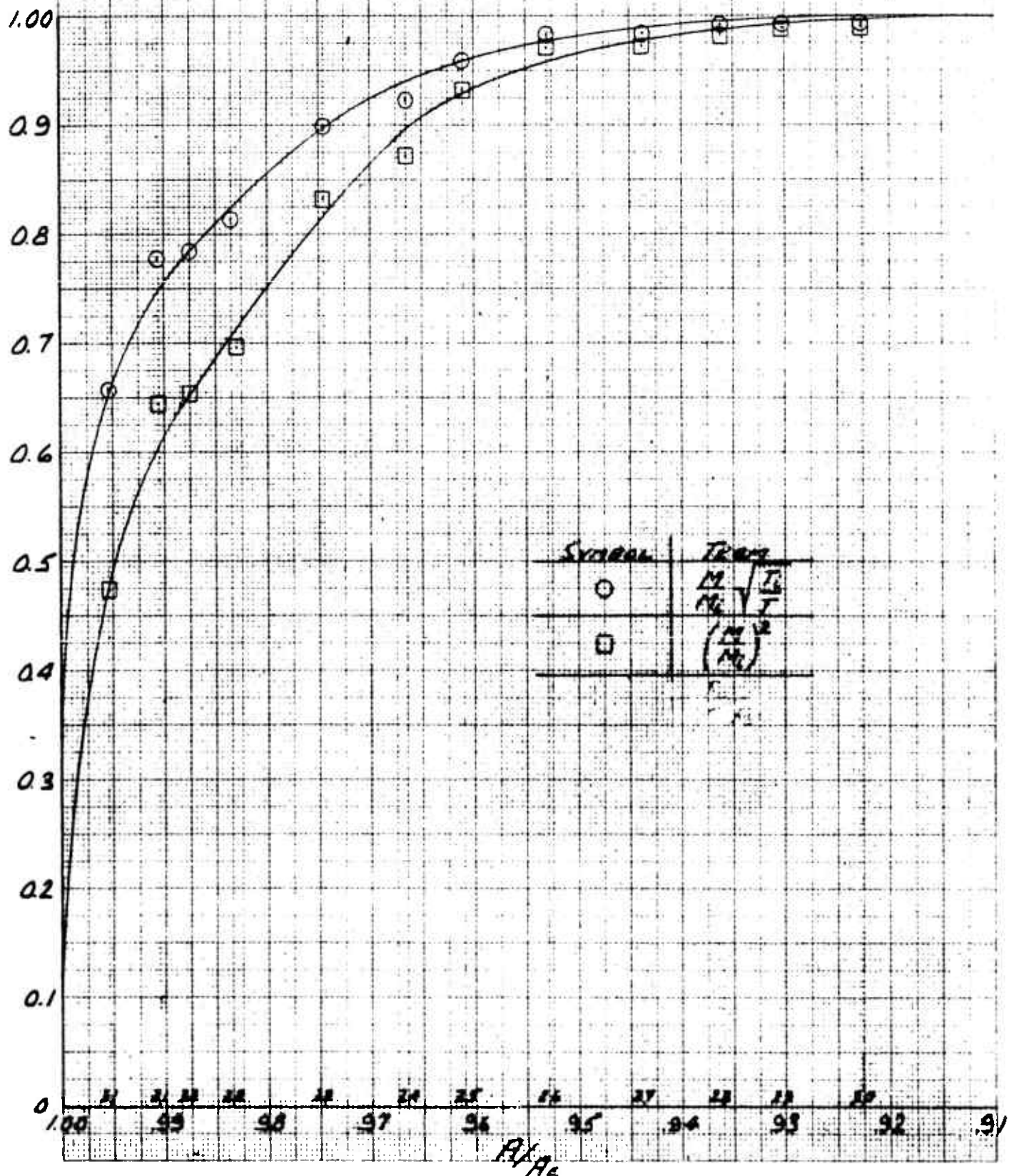
INTEGRATION CURVES
TO DETERMINE C_d & C_v

RUN 16 a DATA POINT 3.985

FLUIDYNE ENGINEERING CORPORATION

8686
Feb 6INTEGRATION CURVES
TO DETERMINE C_d & C_v

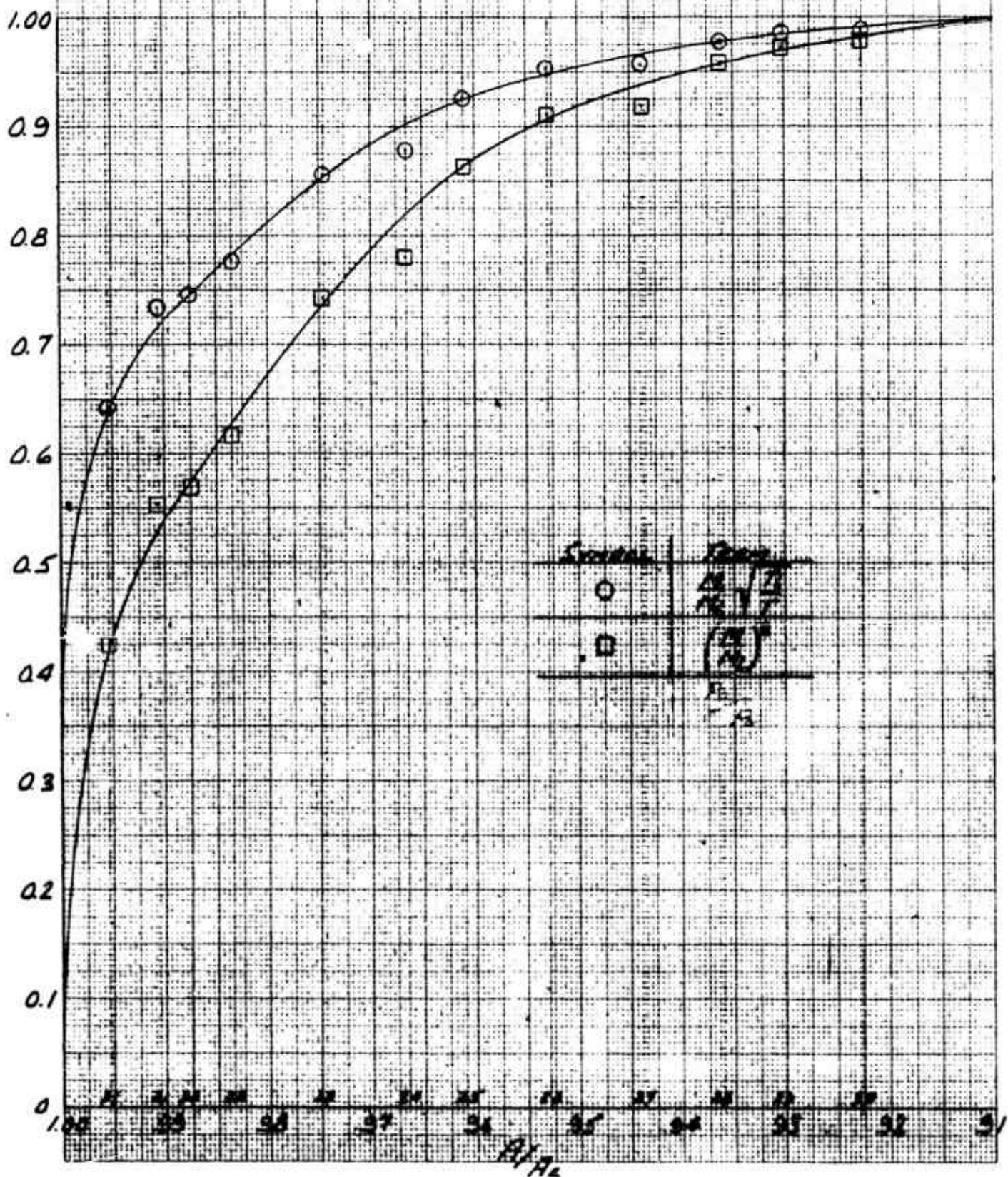
RUN 166 DATA POINT 3.929



FLUIDYNE ENGINEERING CORPORATION

7836
8066INTEGRATION CURVESTO DETERMINE C_d & C_v

RUN 17 DATA POINTS 1.2.192



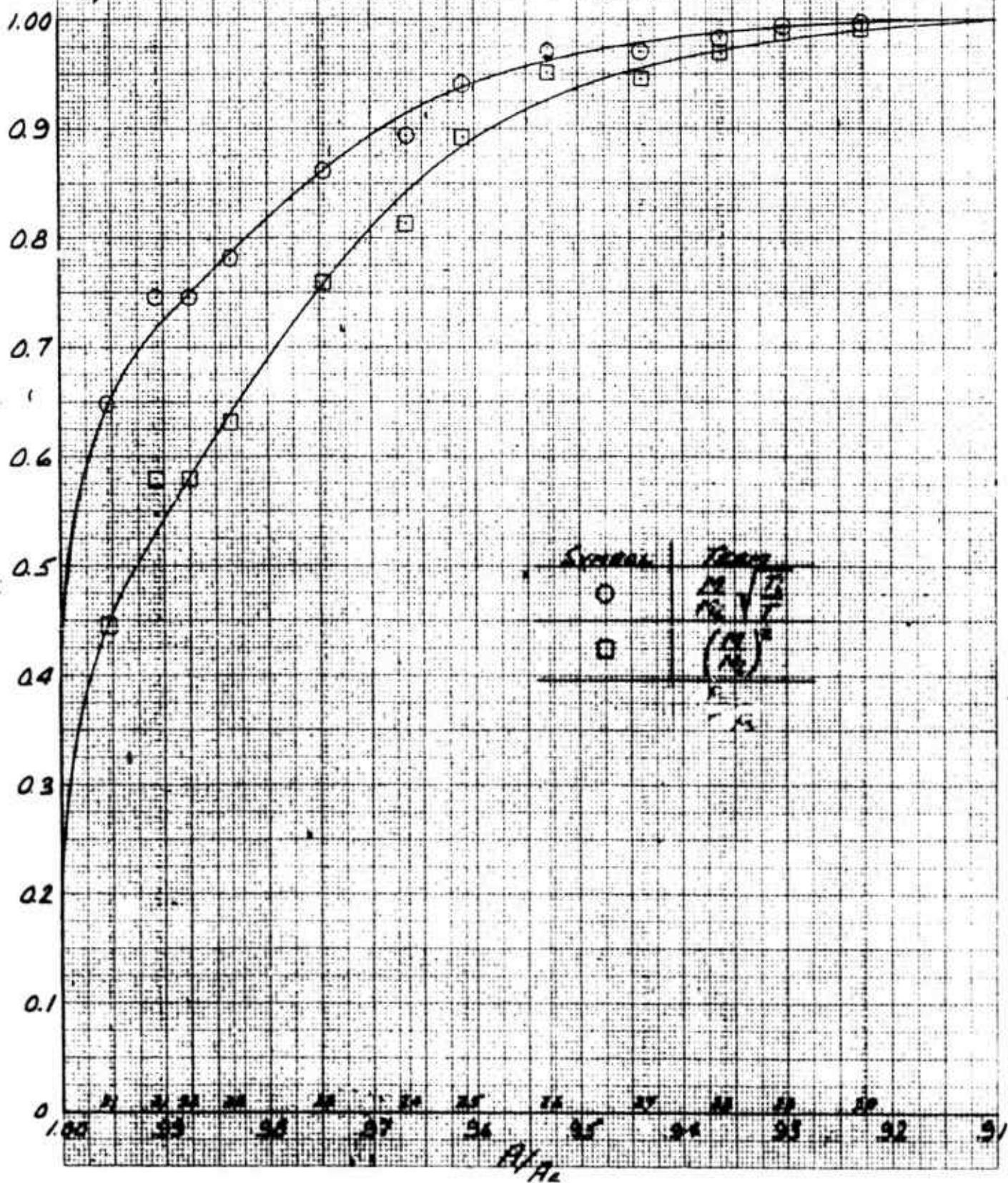
FLUIDYNE ENGINEERING CORPORATION

89/b
11bb

Turbogration Curves

To determine C_d & C_v

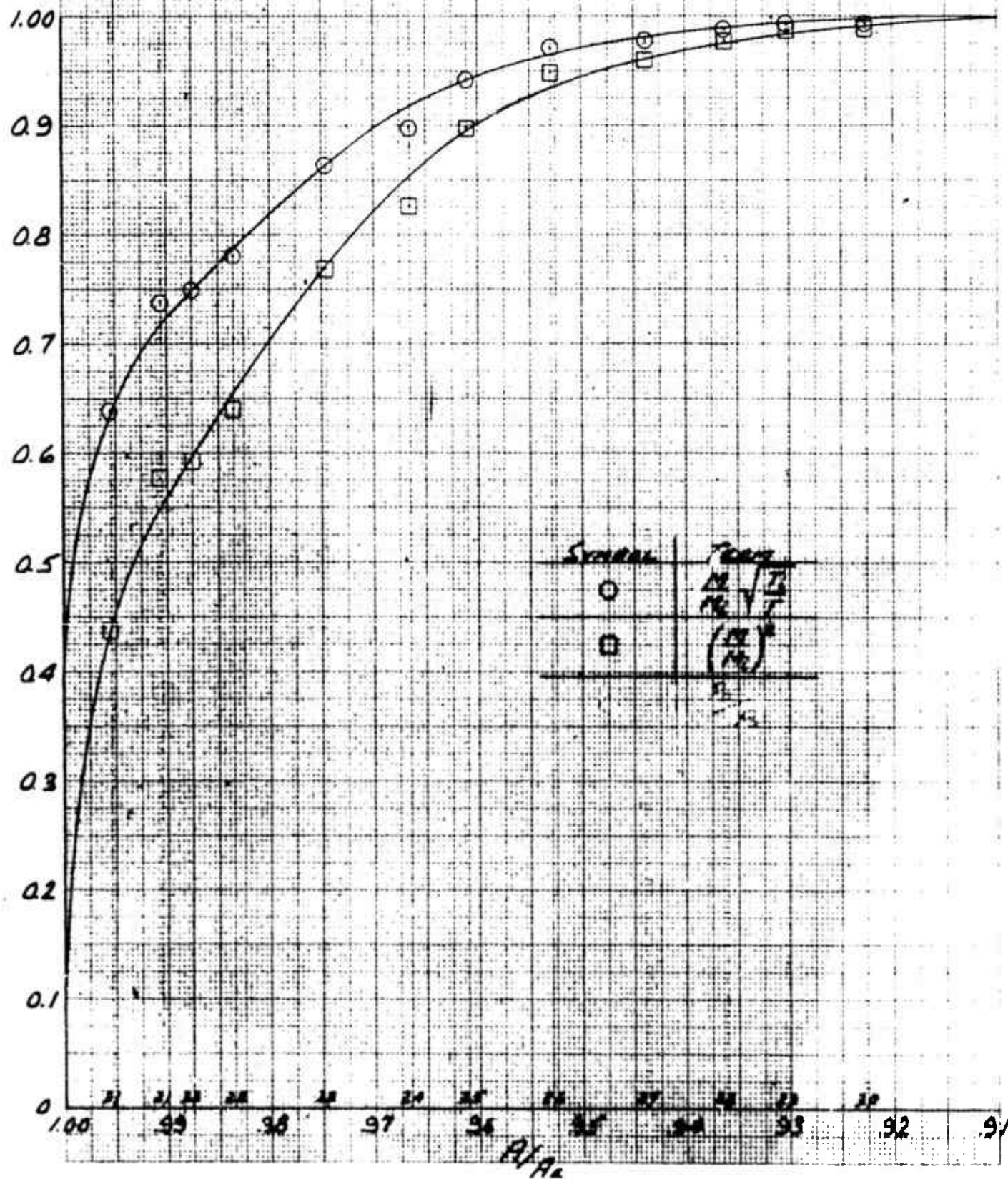
Run 18 DATA POINT 1.4308



FLUIDYNE ENGINEERING CORPORATION

5336
1166INTEGRATION CURVESTO DETERMINE C_0 & C_1

RUN 19 DATA POINT 16472

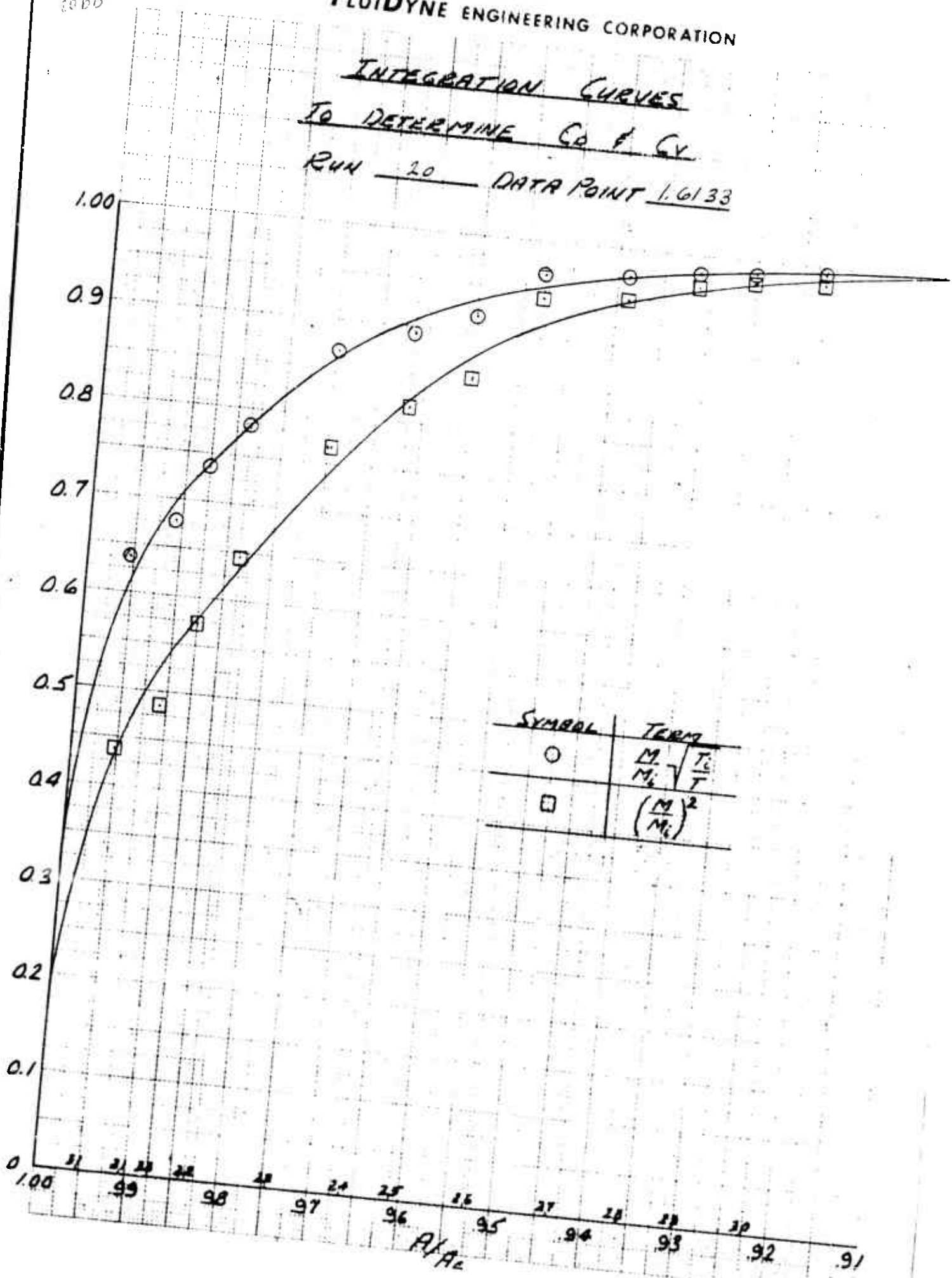


FLUIDYNE ENGINEERING CORPORATION

INTEGRATION CURVES
TO DETERMINE C_D & C_V

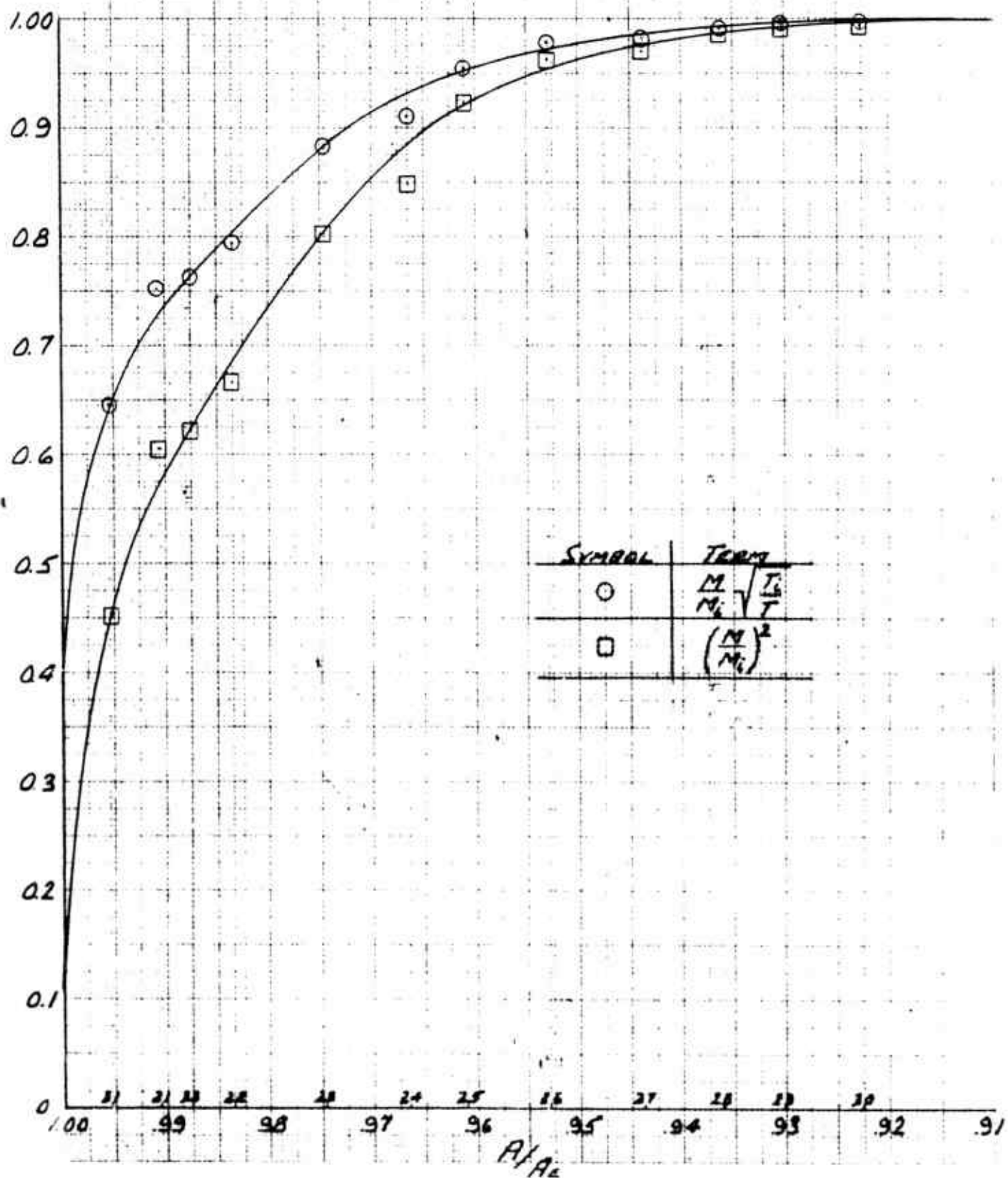
RUN - 20

DATA POINT 1.6133



FLUIDYNE ENGINEERING CORPORATION

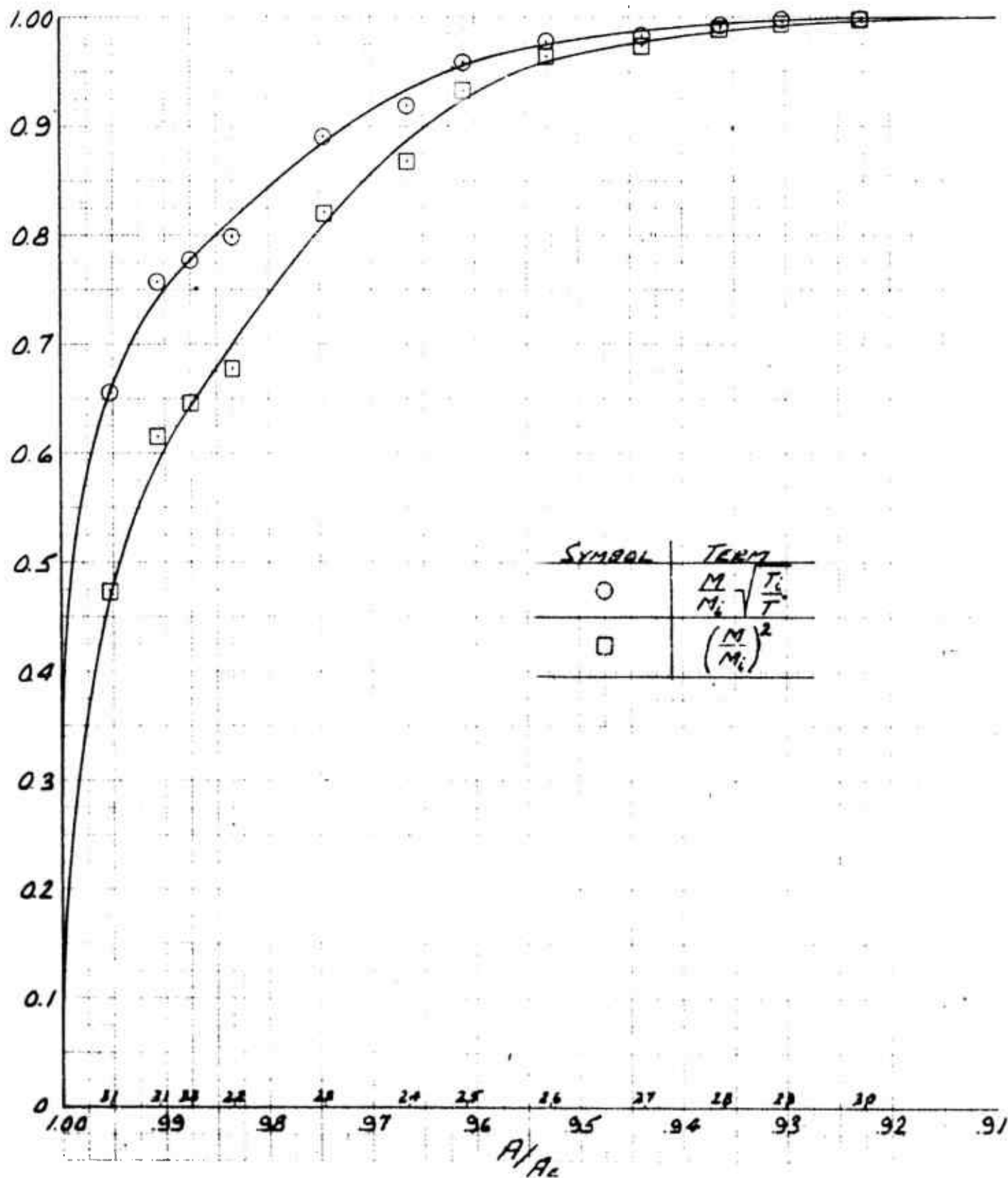
INTEGRATION CURVES
TO DETERMINE C_D & C_V

RUN 21 DATA POINT 1.8586

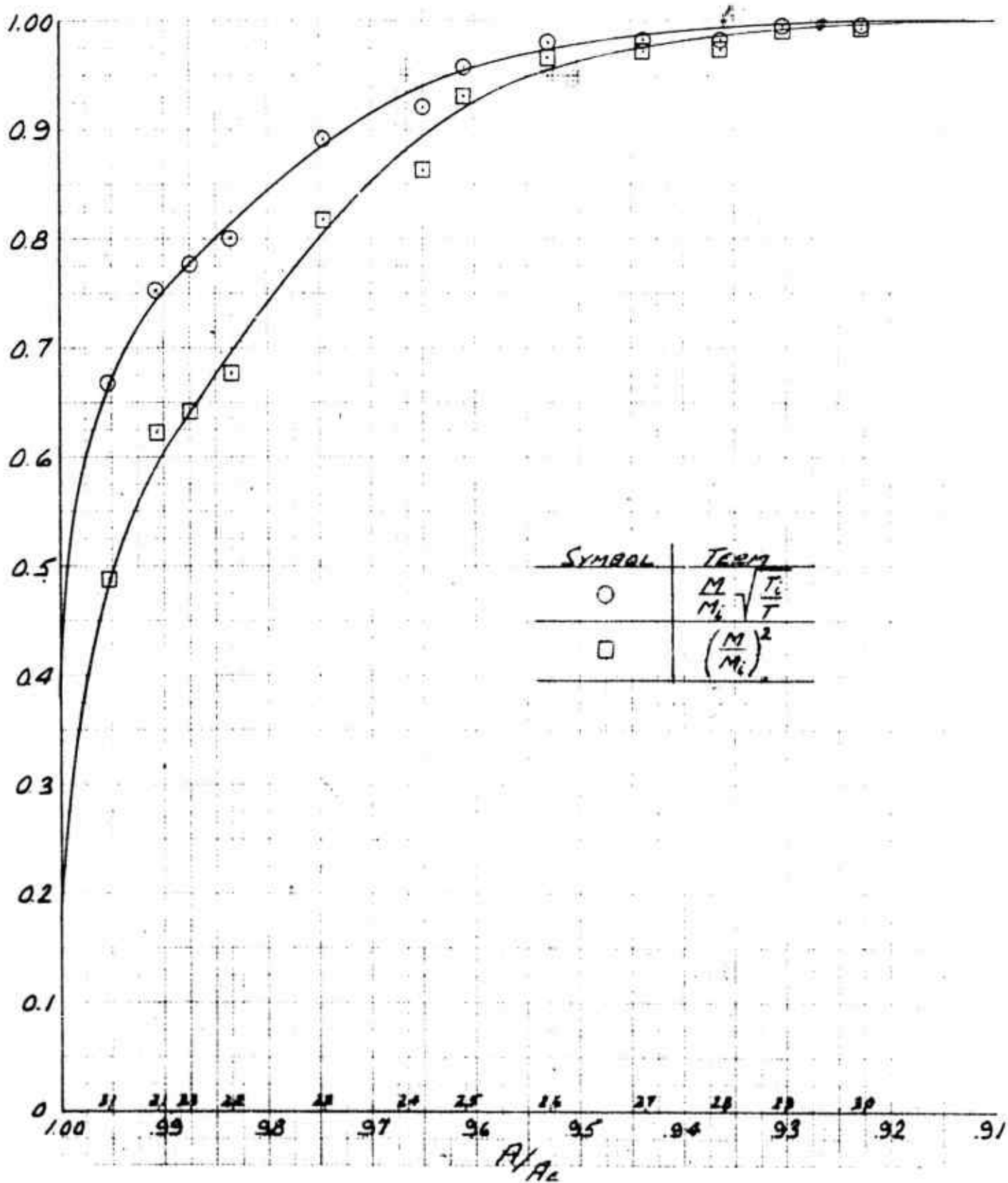
9696
1.66

FLUIDYNE ENGINEERING CORPORATION

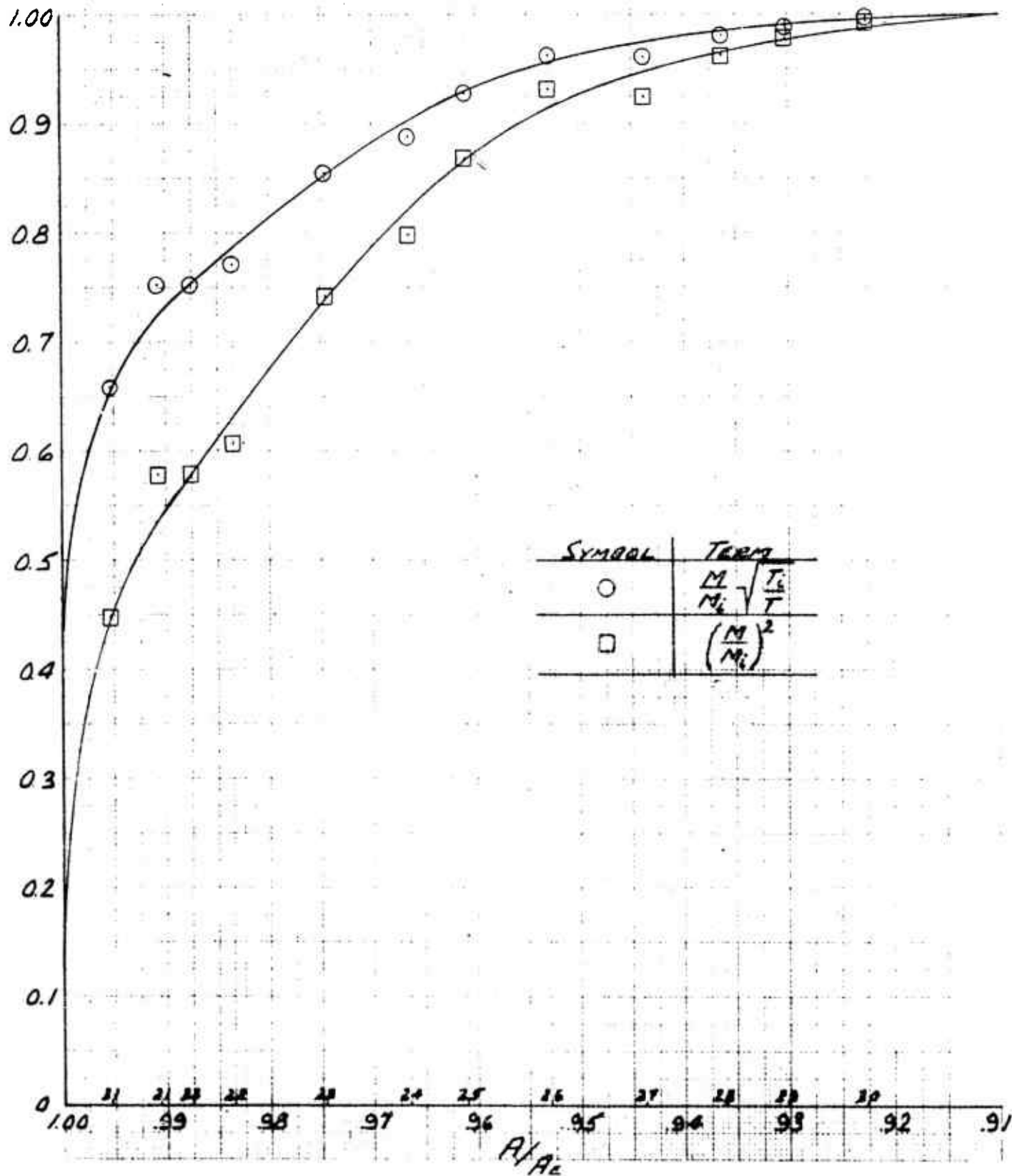
INTEGRATION CURVES
TO DETERMINE C_D & C_V
RUN 22 DATA POINT 2.066



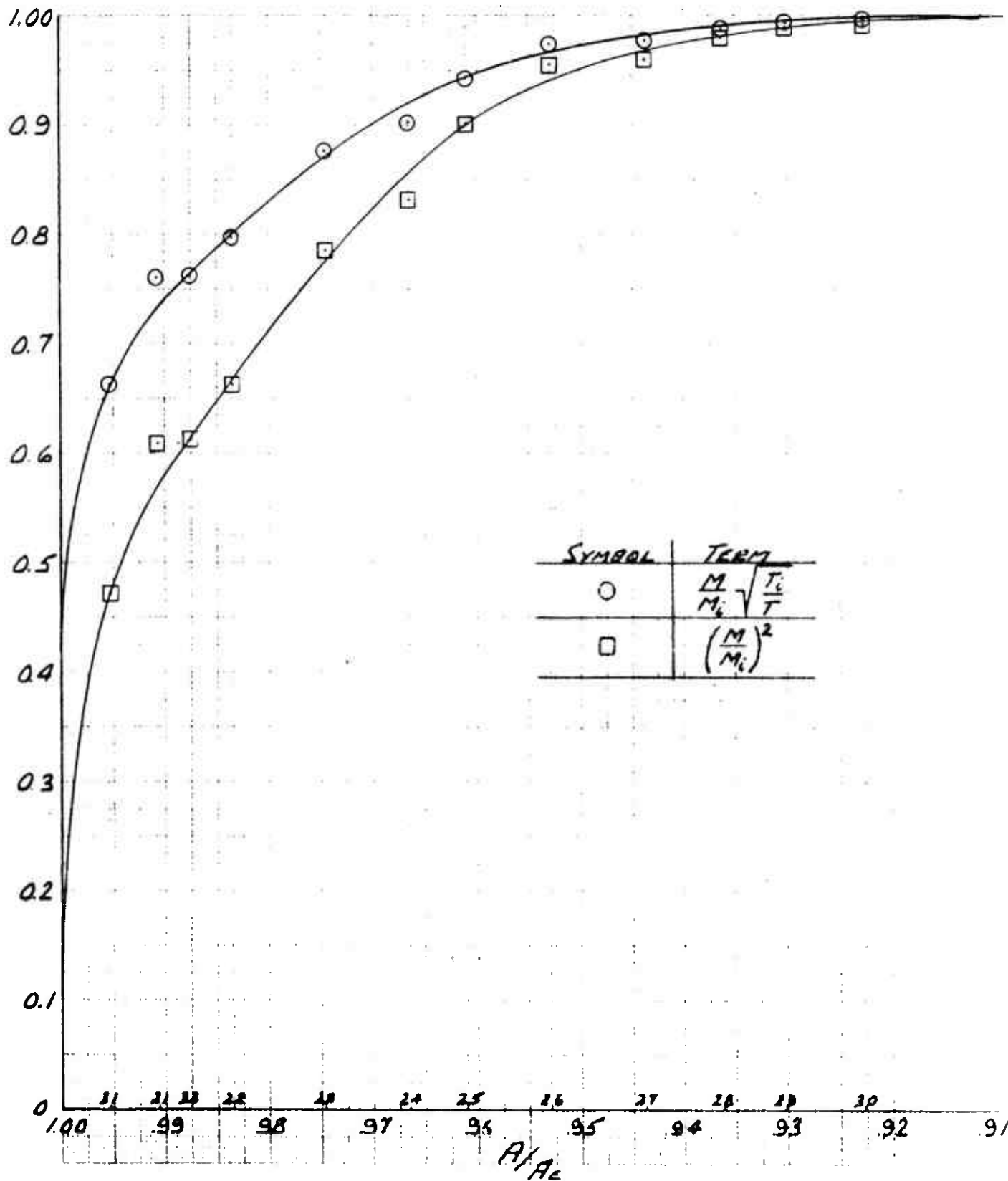
FLUIDYNE ENGINEERING CORPORATION

9186
81bbINTEGRATION CURVESTO DETERMINE C_D & C_V RUN 23 DATA POINT 2.0734

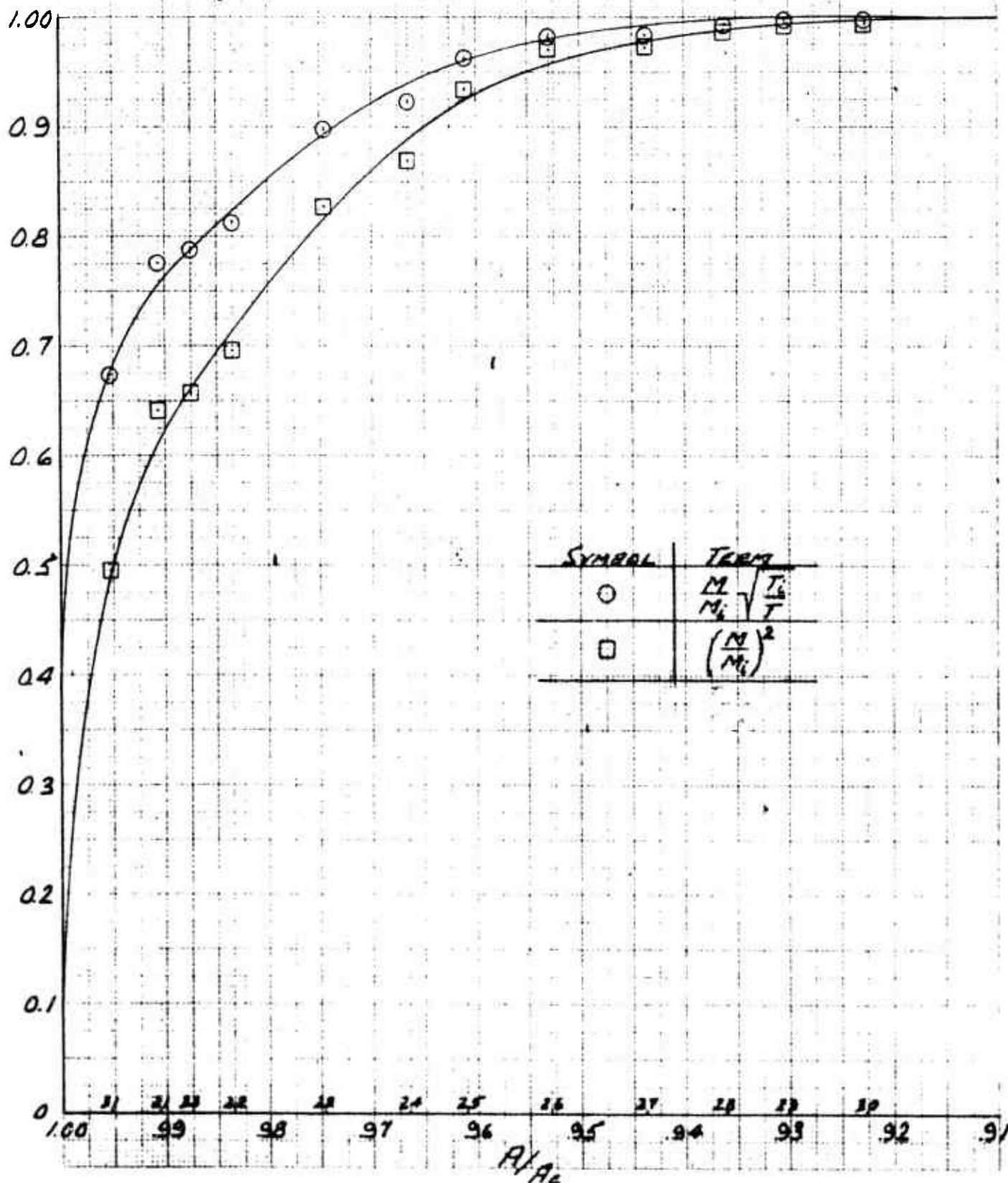
FLUIDYNE ENGINEERING CORPORATION

st 86
gob6INTEGRATION CURVESTO DETERMINE C_D & C_V RUN 24 DATA POINT 1.2133

FLUIDYNE ENGINEERING CORPORATION

J 786
8166INTEGRATION CURVESTO DETERMINE C_D & C_V RUN 25 DATA POINT 1.6171

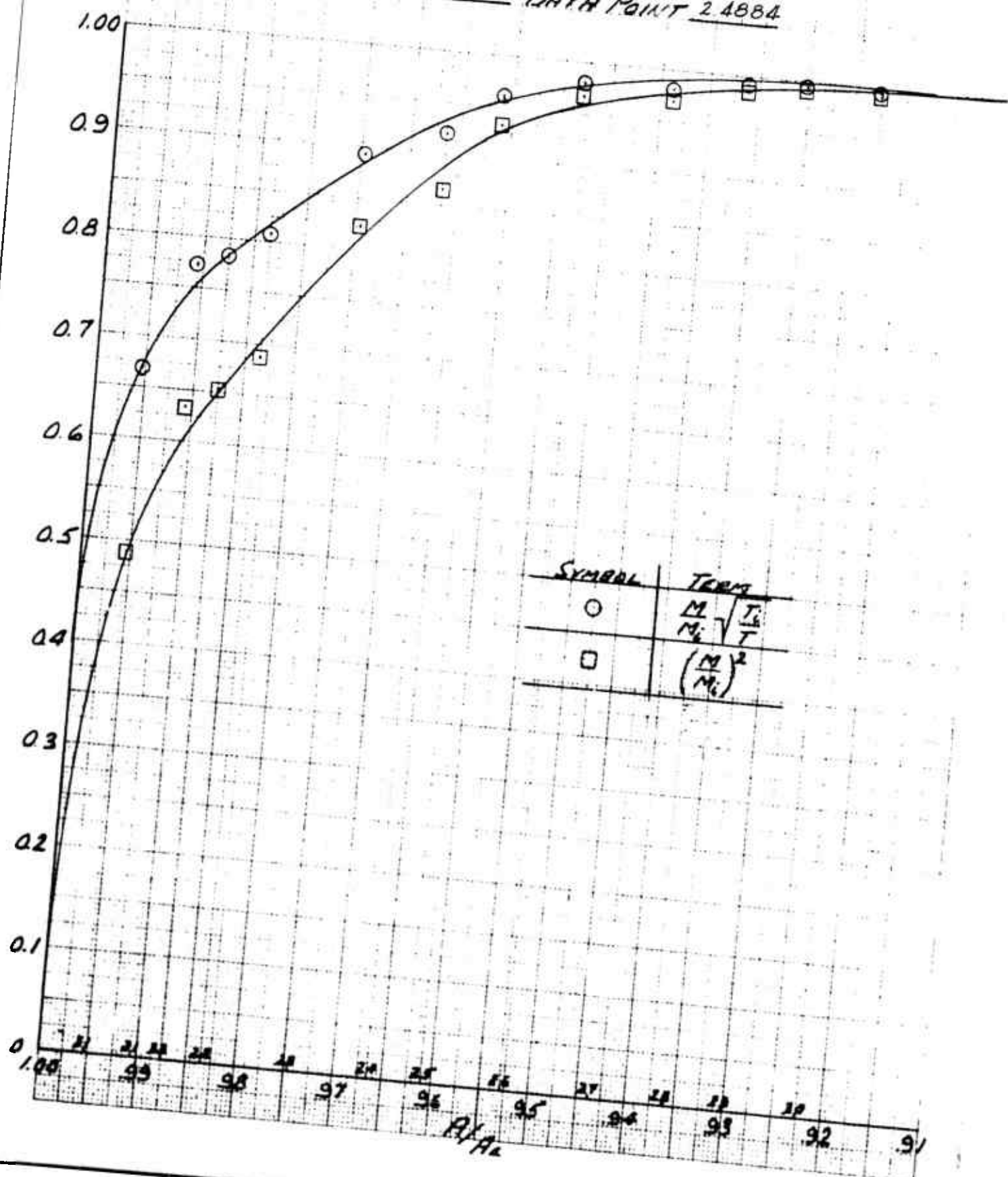
FLUIDYNE ENGINEERING CORPORATION

6L9b.
87bbINTEGRATION CURVESTO DETERMINE C_D & C_V RUN 26 DATA POINT 2.4977

BLB
subb

FLUIDYNE ENGINEERING CORPORATION

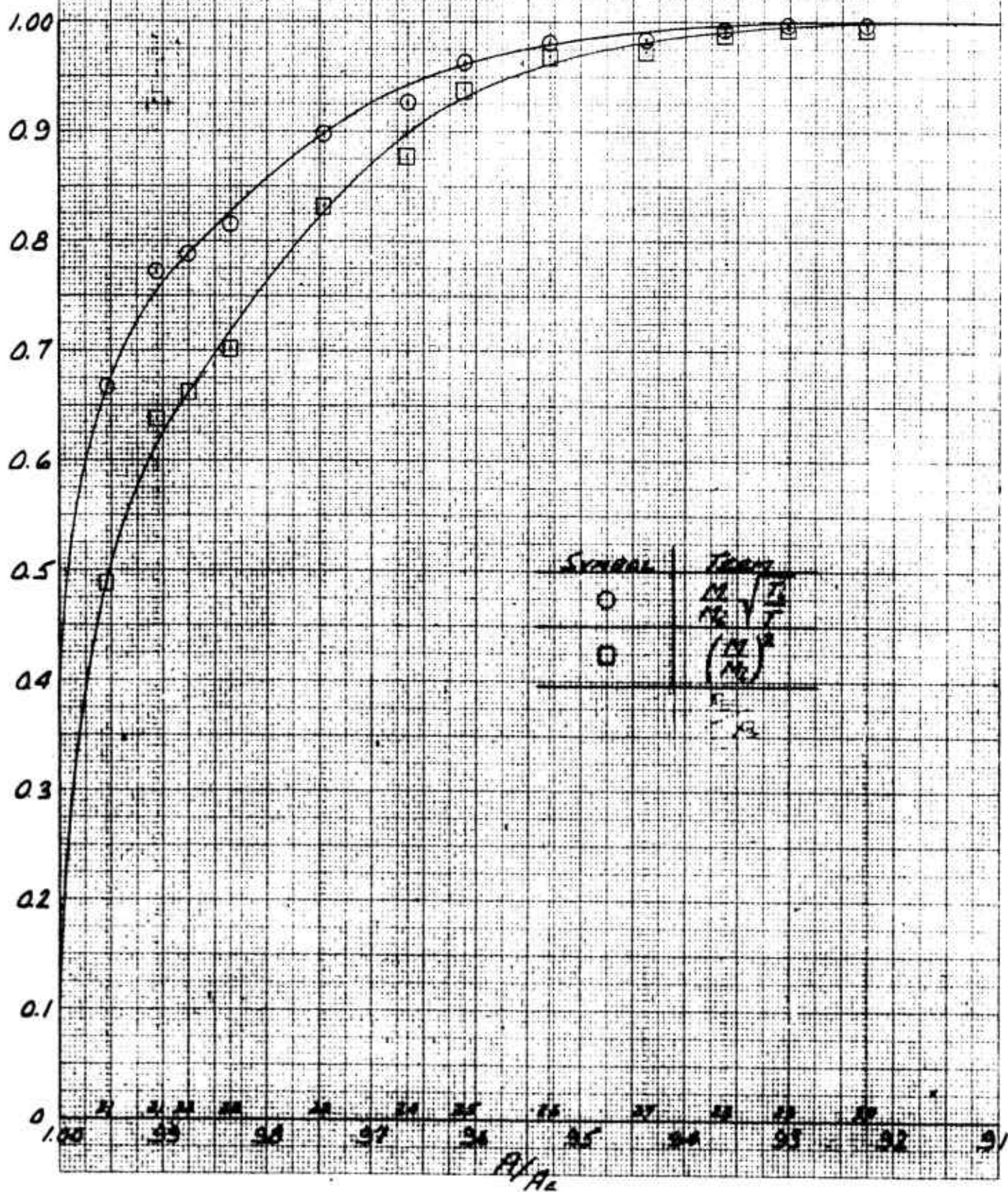
INTEGRATION CURVES
TO DETERMINE C_D & C_V
RUN 27 DATA POINT 24884



FLUIDYNE ENGINEERING CORPORATION

1886
1266INTEGRATION CURVESTO DETERMINE C_0 & C_V

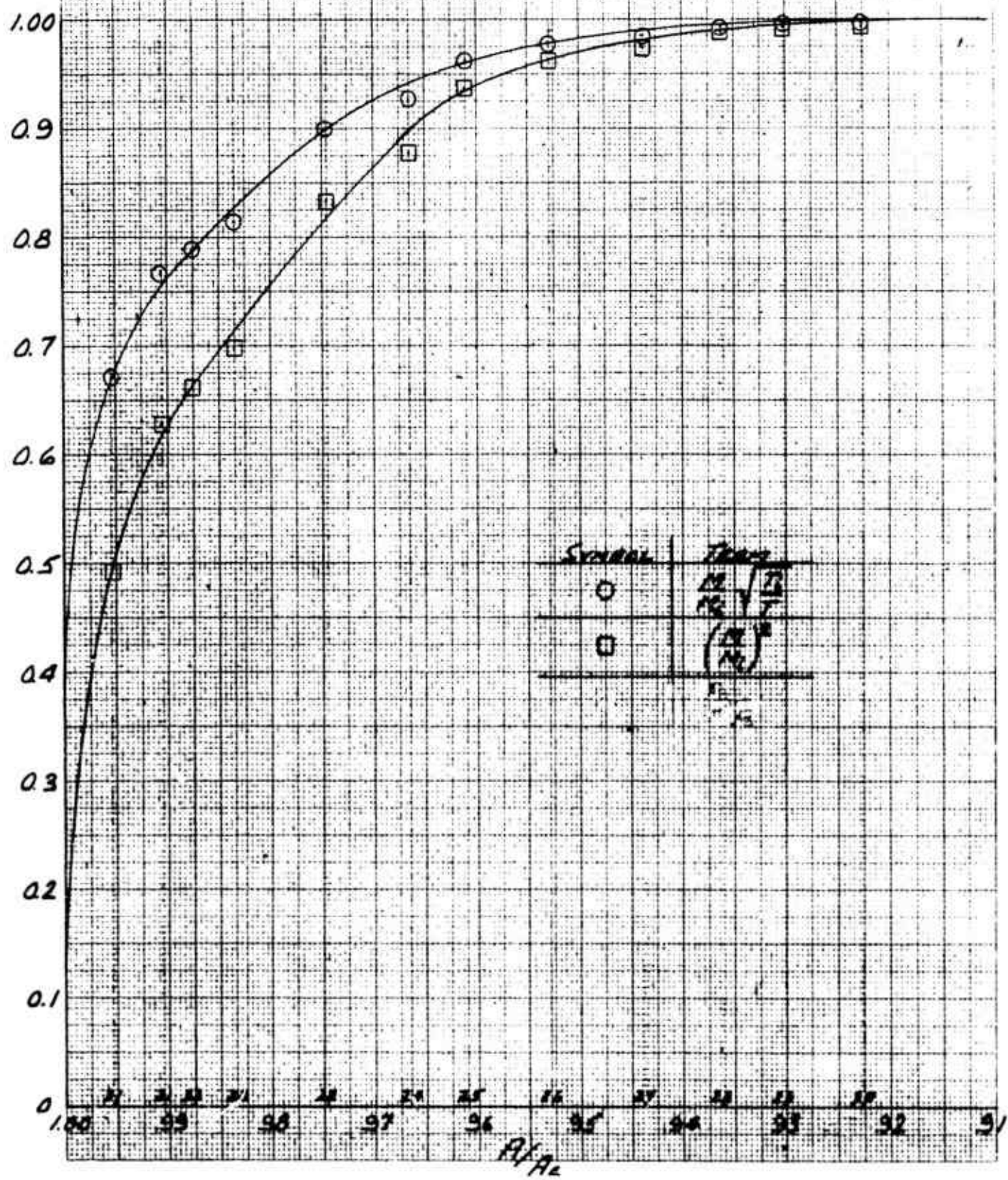
RUN 28 DATA POINT 31284



FLUIDYNE ENGINEERING CORPORATION

2396
8bbbINTEGRATION CurvesTo DETERMINE C_0 & C_1

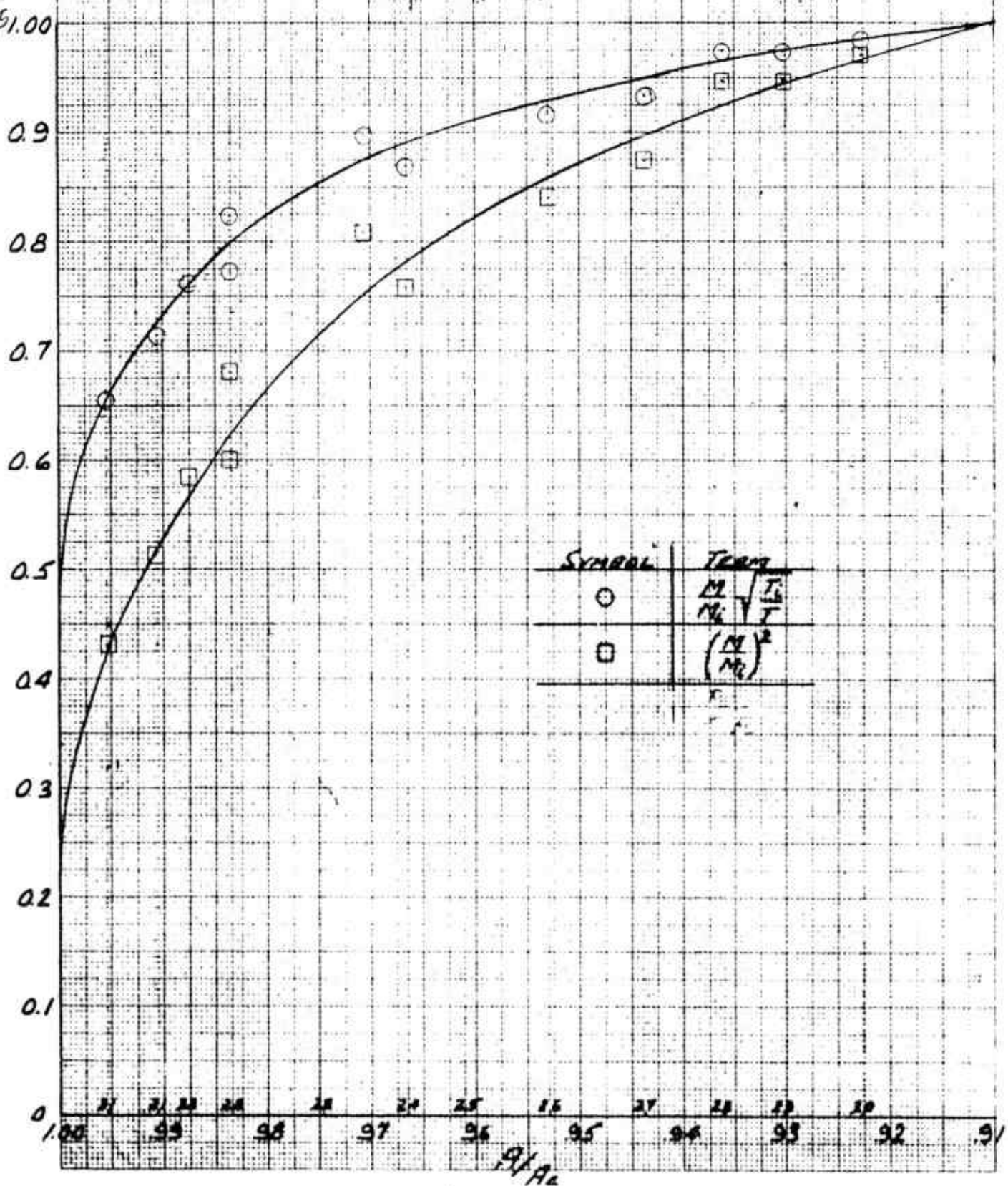
RUN 2.9 DATA POINT 31357



FLUIDYNE ENGINEERING CORPORATION

INTEGRATION CURVESTO DETERMINE C_D & C_V

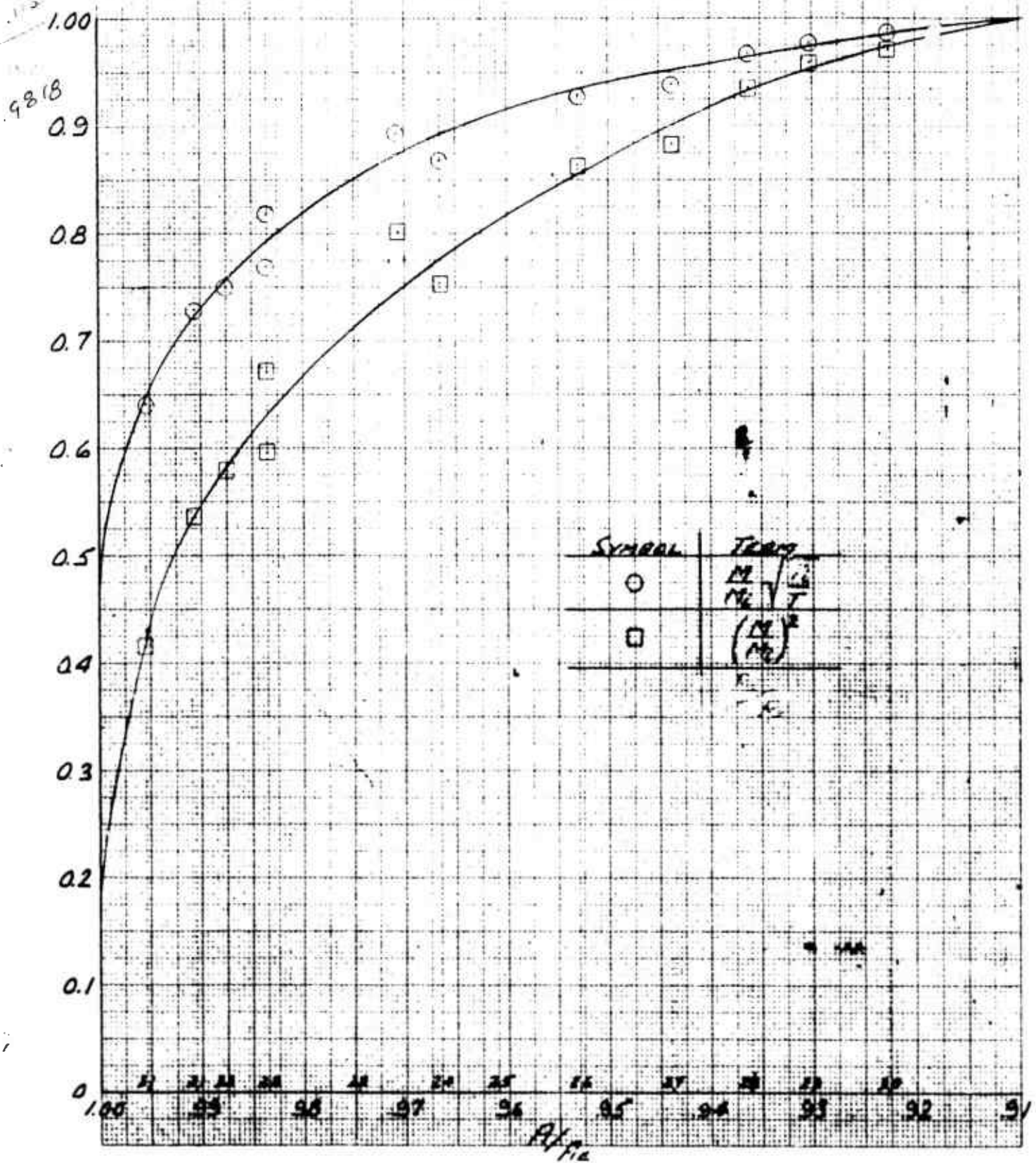
RUN 2-1 DATA POINT 1.0322



FLUIDYNE ENGINEERING CORPORATION

INTEGRATION CURVES
TO DETERMINE C_D & C_V

RUN 2-2 DATA POINT 10529

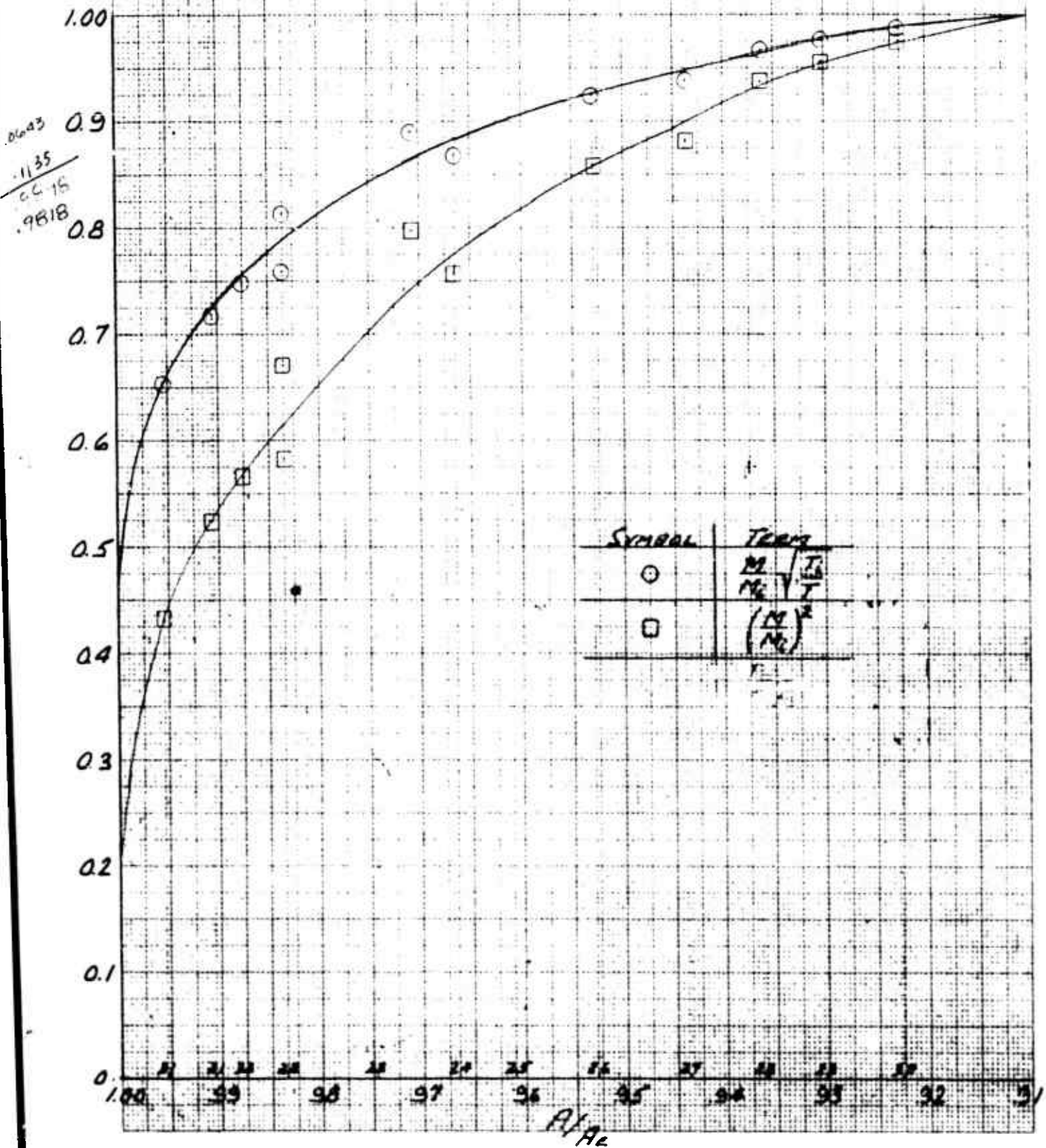


FLUIDYNE ENGINEERING CORPORATION

INTEGRATION CURVES

To DETERMINE C_D & C_V

RUN 2-3 : DATA POINT 1.1062

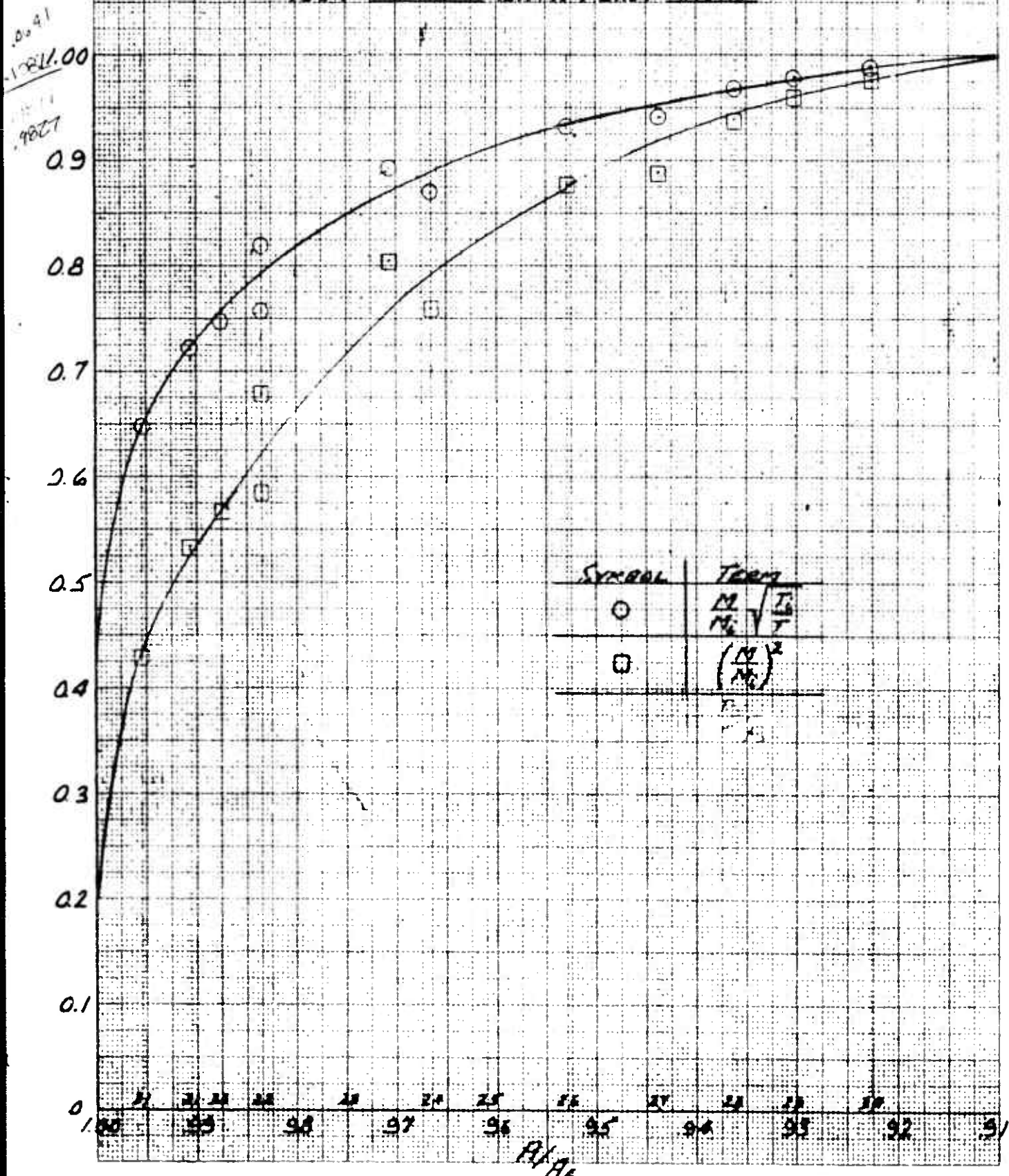


FLUIDYNE ENGINEERING CORPORATION

INTEGRATION CURVES

TO DETERMINE C_D & C_V

RUN 2-4 DATA POINT 11525



FLUIDYNE ENGINEERING CORPORATION

INTEGRATION CURVES
TO DETERMINE C_D & C_V

RUN 2-5 DATA POINT 1/20/18

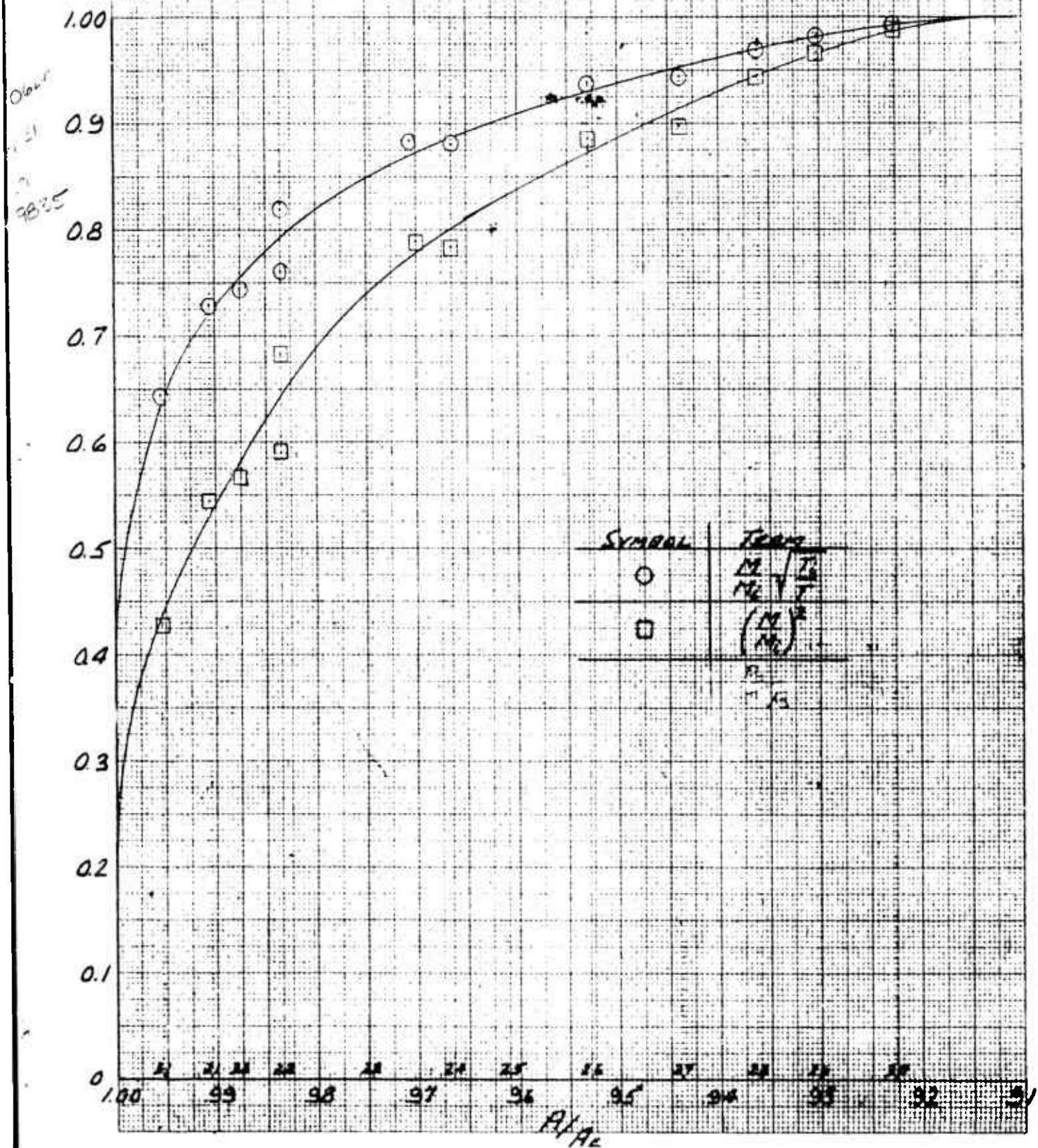


TABLE 1 TABULATED TEST RESULTS

Data Point	Press. Ratio	Po (psia)	Ps (psia)	Pa (psia)	Ps/Pa	$\int \frac{M}{M_1} \sqrt{\frac{T_1}{T}}$	$\frac{dA}{AE}$	$\int \left(\frac{M}{M_1} \right)$
1	1.209	17.23	14.29	14.25	1.0031	.9902		
2	2.408	35.20	18.21	14.25	1.2779	.9923		
3	1.418	20.14	14.28	14.21	1.0052	.9905		
4	1.643	23.34	14.32	14.21	1.0079	.9905		
5	1.857	26.37	14.45	14.21	1.0176	.9915		
6	2.059	29.25	15.41	14.21	1.0848	.9921		
8	2.276	32.23	16.79	14.42	1.1860	.9924		
9	2.487	35.21	18.35	14.42	1.2959	.9925		
10	2.710	38.37	20.02	14.42	1.4141	.9925		
11	2.904	41.05	21.27	14.14	1.5052	.9923		
12	3.120	44.09	22.83	14.13	1.6193	.9925		
13	3.355	47.20	24.57	14.05	1.7491	.9925		
14	3.568	50.10	26.11	14.04	1.8602	.9924		
15	3.773	52.96	27.60	14.04	1.9662	.9926		
16a	3.985	55.93	29.27	14.03	2.0354	.9930		
16b	3.929	55.15	28.79	14.03	2.0513	.9924		
17	1.219	17.12	14.07	14.04	1.0021	.9903		
18	1.431	20.09	14.10	14.04	1.0045	.9911		
19	1.647	23.13	14.13	14.04	1.0066	.9912		
20	1.613	23.14	14.13	14.04	1.0063	.9903		
21	1.859	26.10	14.23	14.04	1.0171	.9917		
22	2.066	29.00	15.25	14.04	1.0361	.9922		
23	2.073	29.11	15.27	14.04	1.0875	.9923		
24	1.213	17.10	14.14	14.09	1.0035	.9903		
25	1.647	23.21	14.43	14.09	1.0278	.9913		
26	2.498	35.20	13.85	14.09	1.3373	.9923		
27	2.488	35.07	13.31	14.09	1.3343	.9925		
28	3.123	44.13	22.94	14.11	1.6260	.9927		
29	3.136	44.24	23.02	14.11	1.6319	.9925		
2-1	1.032	14.055	14.225	14.227	1.00007	.9593		
2-2	1.053	14.930	14.229	14.227	1.00010	.9900		
2-3	1.106	15.733	14.229	14.227	1.00012	.9893		
2-4	1.152	16.397	14.231	14.227	1.00027	.9897		
2-5	1.202	17.099	14.232	14.227	1.00033	.9900		

TEST RESULTS

$\frac{dA}{AE}$	$\int \left(\frac{M}{M_1} \right)^2 \frac{dA}{AE}$	C_D	C_V	C_s	Thrt. Re $\times 10^{-6}$
02	.9829	.9902	.9927	1.1541	2.54
23	.9874	.9923	.9952	1.2689	7.47
05	.9840	.9905	.9953	1.2248	3.62
05	.9851	.9905	.9948	1.2592	4.66
15	.9865	.9915	.9952	1.2683	5.60
21	.9869	.9921	.9953	1.2682	6.19
24	.9879	.9924	.9968	1.2704	6.83
25	.9880	.9925	.9953	1.2680	7.47
25	.9876	.9925	.9941	1.2683	8.15
23	.9878	.9923	.9918	1.2683	8.70
25	.9880	.9925	.9888	1.2704	9.44
25	.9883	.9925	.9880	1.2686	10.0
24	.9880	.9924	.9875	1.2678	10.6
26	.9880	.9926	.9838	1.2681	11.2
30	.9885	.9930	.9819	1.2683	12.0
24	.9873	.9924	.9829	1.2683	11.9
03	.9836	.9903	.9929	1.1593	2.52
11	.9853	.9911	.9938	1.2283	3.62
12	.9855	.9912	.9939	1.2592	4.60
03	.9840	.9903	.9936	1.2587	4.60
17	.9870	.9917	.9954	1.2684	5.54
22	.9376	.9922	.9937	1.2683	6.15
23	.9876	.9923	.9957	1.2711	6.17
08	.9843	.9903	.9939	1.1554	2.53
13	.9354	.9913	.9950	1.2557	4.62
28	.9879	.9928	.9953	1.2681	7.49
25	.9373	.9925	.9955	1.2684	7.43
21	.9882	.9927	.9895	1.2631	4.51
23	.9332	.9925	.9903	1.2679	9.72
93	.9815	.9893	.9921	1.3402	0.94
00	.9818	.9900	.9917	1.0571	1.25
93	.9818	.9893	.9919	1.0968	1.73
97	.9827	.9897	.9929	1.1251	2.11
00	.9835	.9900	.9934	1.1523	2.42

2